

AIRBORNE SUSPENSION/VIBRATION ISOLATION SYSTEM

David A. Kienholz

CSA Engineering, Inc.
2850 West Bayshore Road
Palo Alto, CA 94303-3843

August 1996

Final Report

Distribution authorized to DoD components only; Proprietary Information; August 1996. Other requests for this document shall be referred to Phillips Laboratory, 3550 Aberdeen Ave. SE, Kirtland AFB, NM 87117-5776.

WARNING - This document contains technical data whose export is restricted by the Arms Export Control Act (Title 22, U.S.C., Sec 2751 et seq.) or The Export Administration Act of 1979, as amended (Title 50, U.S.C., App. 2401, et seq.). Violations of these export laws are subject to severe criminal penalties. Disseminate IAW the provisions of DoD Directive 5230.25 and AFI 61-204.

DESTRUCTION NOTICE - For classified documents, follow the procedures in DoD 5200.22-M, Industrial Security Manual, Section II-19 or DoD 5200.1-R, Information Security Program Regulation, Chapter IX. For unclassified, limited documents, destroy by any method that will prevent disclosure of contents or reconstruction of the document.



PHILLIPS LABORATORY
Space Technology Directorate
AIR FORCE MATERIEL COMMAND
KIRTLAND AIR FORCE BASE, NM 87117-5776

DTIC QUALITY INSPECTED 2

19970221 028

UNCLASSIFIED



AD NUMBER

AD-B220 493

NEW LIMITATION CHANGE

TO

DISTRIBUTION STATEMENT A -
Approved for public release; Distri-
bution unlimited.

Limitation Code: 1

FROM

DISTRIBUTION STATEMENT -

Limitation Code:

AUTHORITY

Jarvis E. Mosher; Phillips Lab/CA, Kirtland AFB,
N.M.

THIS PAGE IS UNCLASSIFIED

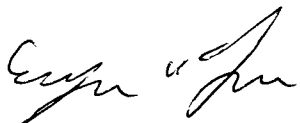
Using Government drawings, specifications, or other data included in this document for any purpose other than Government procurement does not in any way obligate the U.S. Government. The fact that the Government formulated or supplied the drawings, specifications, or other data, does not license the holder or any other person or corporation; or convey any rights or permission to manufacture, use, or sell any patented invention that may relate to them.

This report contains proprietary information and shall not be either released outside the government, or used, duplicated or disclosed in whole or in part for manufacture or procurement, without the written permission of the contractor. This legend shall be marked on any reproduction hereof in whole or in part.

If you change your address, wish to be removed from this mailing list, or your organization no longer employs the addressee, please notify PL/VTV, 3550 Aberdeen Ave SE, Kirtland AFB, NM 87117-5776.

Do not return copies of this report unless contractual obligations or notice on a specific document requires its return.

This report has been approved for publication.



EUGENE FOSNESS
Project Manager

FOR THE COMMANDER



L. KEVIN SLIMAK, GM-15
Chief, Space Vehicle Technologies
Division



CHRISTINE M. ANDERSON
Director, Space Technology
Directorate

The following notice applies to any unclassified (including originally classified and now declassified) technical reports released to "qualified U.S. contractors" under the provisions of DoD Directive 5230.25, Withholding of Unclassified Technical Data From Public Disclosure.

NOTICE TO ACCOMPANY THE DISSEMINATION OF EXPORT-CONTROLLED TECHNICAL DATA

1. Export of information contained herein, which includes, in some circumstances, release to foreign nationals within the United States, without first obtaining approval or license from the Department of State for items controlled by the International Traffic in Arms Regulations (ITAR), or the Department of Commerce for items controlled by the Export Administration Regulations (EAR), may constitute a violation of law.
2. Under 22 U.S.C. 2778 the penalty for unlawful export of items or information controlled under the ITAR is up to two years imprisonment, or a fine of \$100,000, or both. Under 50 U.S.C., Appendix 2410, the penalty for unlawful export of items or information controlled under the EAR is a fine of up to \$1,000,000, or five times the value of the exports, whichever is greater; or for an individual, imprisonment of up to 10 years, or a fine of up to \$250,000, or both.
3. In accordance with your certification that establishes you as a "qualified U.S. Contractor", unauthorized dissemination of this information is prohibited and may result in disqualification as a qualified U.S. contractor, and may be considered in determining your eligibility for future contracts with the Department of Defense.
4. The U.S. Government assumes no liability for direct patent infringement, or contributory patent infringement or misuse of technical data.
5. The U.S. Government does not warrant the adequacy, accuracy, currency, or completeness of the technical data.
6. The U.S. Government assumes no liability for loss, damage, or injury resulting from manufacture or use for any purpose of any product, article, system, or material involving reliance upon any or all technical data furnished in response to the request for technical data.
7. If the technical data furnished by the Government will be used for commercial manufacturing or other profit potential, a license for such use may be necessary. Any payments made in support of the request for data do not include or involve any license rights.
8. A copy of this notice shall be provided with any partial or complete reproduction of these data that are provided to qualified U.S. contractors.

D E S T R U C T I O N N O T I C E

For classified documents, follow the procedures in DoD 5200.22-M, Industrial Security Manual, Section II-19 or DoD 5200.1-R, Information Security Program Regulation, Chapter IX. For unclassified, limited documents, destroy by any method that will prevent disclosure of contents or reconstruction of the document.

DRAFT SF 298

1. Report Date (dd-mm-yy) August 1996		2. Report Type Final		3. Dates covered (from... to) 11/93 to 08/96	
4. Title & subtitle Airborne Suspension/Vibration Isolation System			5a. Contract or Grant # F29601-93-C-0203		
			5b. Program Element # 62601F		
6. Author(s) David A. Kienholz			5c. Project # 3005		
			5d. Task # C0		
			5e. Work Unit # CY		
7. Performing Organization Name & Address CSA Engineering, Inc. 2850 West Bayshore Road Palo Alto, CA 94303-3843				8. Performing Organization Report # 96-08-03	
9. Sponsoring/Monitoring Agency Name & Address Phillips Laboratory 3550 Aberdeen Ave. SE Kirtland AFB, NM 87117-5776				10. Monitor Acronym	
				11. Monitor Report # PL-TR-96-1130	
12. Distribution/Availability Statement Distribution authorized to DoD components only; Proprietary Information; August 1996. Other requests for this document shall be referred to Phillips Laboratory, 3550 Aberdeen Ave. SE, Kirtland AFB, NM 87117-5776.					
13. Supplementary Notes					
14. Abstract A hybrid passive-active vibration isolation system for airborne optical systems is described. Designed for the requirements of the Air Force Airborne Laser program, it uses an advanced semipassive system of pneumatic mounts to support the payload weight with very low stiffness and hysteresis. Horizontal isolation is accommodated by passive means using all-metal flexures. High-force voice coil actuators act on the payload in all six degrees of freedom with vertical actuators integrated into the pneumatic counts. The passive system provides isolation break frequencies of 0.6-1.25 Hz with vertical isolation of -40 dB at frequencies as low as 4.0 Hz. A real-time control processor allows the active subsystem to provide a number of performance enhancements. It can reduce static sag and sway during aircraft maneuvering, can damp the passive system, and can provide inertial stabilization of the entire optical platform during level flight. Design and construction of a proof-of-concept demonstration system are described along with methods and results for system-level and component-level tests.					
15. Subject Terms Vibration; isolation; active control; airborne optics; airborne laser					
Security Classification of			19. Limitation of Abstract limited	20. # of Pages 72	21. Responsible Person (Name and Telephone #) Eugene Fosness (505) 846-7883
16. Report Unclassified	17. Abstract Unclassified	18. This Page Unclassified			

Government Purpose License Rights Legend

Contract No. F29601-93-C-0203

Contractor: CSA Engineering, Palo Alto, CA

Government purpose license rights shall be effective until December 2000; thereafter, the Government purpose license rights will expire and the Government shall have unlimited rights in the technical data. The restrictions governing use of technical data marked with this legend are set forth in the definition of "Government Purpose License Rights" in paragraph (a)(14) of the clause at 252.227-7013 of the contract listed above. This legend, together with the indications of the portions of this data which are subject to Government purpose license rights, shall be included on any reproduction hereof which includes any part of the portions subject to such limitations.

Export Control Warning:

"WARNING THIS DOCUMENT MAY CONTAIN TECHNICAL DATA WHOSE EXPORT IS RESTRICTED BY THE ARMS EXPORT CONTROL ACT (Title 22, USC Sec 2751, et seq) OR THE EXPORT ADMINISTRATION ACT OF 1979, as amended, Title 50, USC Aop 2401 et seq. VIOLATIONS OF THESE EXPORT LAWS ARE SUBJECT TO SEVERE CRIMINAL PENALTIES. Disseminate I.A.W. the provisions of DOD Directive 5230.25.

SBIR Proprietary Data

This report contains proprietary data which was generated under the terms of a Federal Small Business Innovation Research (SBIR) contract. All such data is proprietary to the contractor for a period of four years after completion of the project (Public Law 102-564). This data shall not be released outside the Department of Defense (DOD), or used, duplicated, or disclosed in whole or in part for manufacture or procurement, without the express written permission of the contractor.

This report documents the SBIR Phase II development of a vibration isolation system for use with airborne optical systems. In addition to the report author, others working on the project included the following. Mr. Bryce Fowler of CSA developed the real-time control software. Mr. Scott Pendleton of CSA performed the design analysis of magnetic actuators, designed the test apparatus, and assisted in system assembly and test. Mr. Mike Evert of CSA assembled the AS/VIS isolation mounts and actuators and the system test apparatus. Mr. Mike Huber of MSH Engineering performed detail mechanical design and fabrication of the isolators and actuators. The work was performed under contract No. F29601-93-C-0203.

Prepared by: David A. Kienholz
David A. Kienholz
Principal Engineer

Contents

1. Introduction, Background, and Summary	1
1.1 Isolation for ABL Optical Benches	2
1.2 Technology Base	4
1.3 Summary of Accomplishments	4
2. Design Description	9
2.1 Concept and Operating Principle	9
2.2 Vertical Airmount/Actuator	10
2.3 Horizontal Actuator	14
2.4 Magnetic Actuators	16
2.5 Analog Electronics	20
2.5.1 Acceleration Sensing	20
2.5.2 Position Sensing	24
2.5.3 Power Preamps and Amplifiers	26
2.6 Digital Control Hardware and Software	29
3. Test Methods and Results	32
3.1 Actuator Tests	32
3.2 System Test Apparatus	35
3.3 System-Level Isolation Tests	37
3.4 Other System Level Tests	40
3.5 Component-level Isolation Tests	41
3.5.1 Test Method	42
3.5.2 Test Apparatus and Procedure	44
3.5.3 Instrumentation	44
3.5.4 Test Procedure	45
3.5.5 Results	46
3.6 Test Conclusions	51
4. Control Laws	53
4.1 Acceleration Feedforward	53
4.2 Positive Position Feedback	55
4.3 Inertial Stabilization	55

5. Conclusions	59
5.1 Suggested Future Work	59
5.2 Evolution to Flight Systems	60

List of Figures

1	Pneumatic vs. linear elastic vibration mounts	2
2	Pneumatic-magnetic suspension devices for zero-g simulation	5
3	AS/VIS demonstration testbed. The entire system is sized for payloads heavier than the currently expected weights of the Airborne Laser optical benches.	6
4	AS/VIS simplified operating principle	10
5	Vertical airmount with integral voice-coil actuator	11
6	Vertical airmount subassemblies	12
7	Horizontal voice-coil actuator	15
8	Demagnetization curve for magnet material (top) and BH curve for back-iron material (bottom)	18
9	Calculated flux field at symmetry plane of voice coil actuator magnet assembly.	19
10	Calculated force vs. coil position for magnetic actuator.	19
11	Actuator coil design. Some data are as-measured from prototype coil.	21
12	16-channel accelerometer chassis.	23
13	Accelerometer signal chain.	24
14	Accelerometer locations.	25
15	Chassis for 8-channel displacement signal conditioning and power preamplifiers.	27
16	Power preamplifier and amplifier simplified schematic.	28
17	8-channel power amplifier panel and amplifier module.	29
18	Frequency response of current-drive power amplifier.	30
19	Block diagram of real-time control processor and development system.	32
20	Testing of horizontal actuator.	33
21	Static test results for horizontal actuator.	34
22	Dynamic test results for horizontal actuator.	35
23	System-level test apparatus.	36
24	Test setup schematic.	38
25	0.5-40 Hz system-level test results.	39
26	0.5-9.0 Hz system-level test results.	40
27	Laser beams from platform and payload under 10-Hz sine excitation.	41
28	Direct (left) and indirect (right) methods of testing isolator transmissibility.	43

29	Test apparatus for single-unit vertical transmissibility testing. Device carriages are shown in light grey and load plates in darker gray. . . .	45
30	Test matrix for component-level isolation tests.	47
31	Measured single-dof transmissibility with 353-lb payload.	48
32	Measured single-dof transmissibility with 195-lb payload.	49
33	Typical input and output acceleration spectra from component transmissibility tests.	50
34	Calculated and measured vertical suspension frequencies.	51
35	6-DOF control law using pneumatic airmounts, vertical displacement feedback, passive horizontal springs, and floor acceleration feedforward.	54
36	Simplified acceleration feedforward control law for one degree of freedom.	56
37	Payload absolute acceleration (top) and isolator displacement (bottom) for three types of isolators. 1 - AS/VIS with acceleration feedforward, 2 - AS/VIS without acceleration feedforward, 3 - 3.0 Hz passive with 10% damping.	57

1. Introduction, Background, and Summary

This report documents the SBIR Phase II development of a unique passive-active vibration isolation system for sensitive airborne payloads such as optical benches. The system, called the Airborne Suspension/Vibration Isolation System (AS/VIS) is designed for the special requirements of the Airborne Laser (ABL).

The Air Force Airborne Laser program will in late 1996 begin full-scale development of a powerful laser and associated pointing and tracking systems for use at high altitudes in a Boeing 747 aircraft. The laser weapon is intended for use against tactical surface-to-surface missiles during boost phase. During the course of this SBIR Phase II development, the evolving AS/VIS design became a baseline element of the design of Team ABL, the Boeing-Lockheed Martin-TRW team which won the Airborne Laser competition. Phase III development will therefore be carried out within the ABL program, where two derivatives of AS/VIS will be used in the the prototype ABL aircraft.

AS/VIS has reached the stage of laboratory demonstration hardware. It has been designed as, among other things, a laboratory tool for efficient development of flightworthy ABL isolation systems based on AS/VIS. The testbed hardware will be turned over to the Phillips Laboratory for use, either by the Air Force or its contractors, in this continuing development process.

CSA Engineering is a member of Team ABL. In addition to isolation system development, CSA will perform a variety of engineering work within the ABL program. As a team member, CSA had access to engineering data on the overall design that was relevant to requirements for the bench isolation systems. For proprietary reasons, all such data was excluded from this report, most of which was written prior to the announcement of the ABL contract winner. Fortunately, this deliberate omission does not compromise the purpose of the report. AS/VIS has, from the beginning, been designed as a technology-push rather than requirements-pull development¹. That is, the SBIR Phase II objective was to develop the most capable isolation system possible, even if it exceeded the actual requirements for ABL as they evolved. Besides satisfying the objective of risk reduction, this technology-push approach was motivated by practical reasons. The ABL teams had not even been formed when the plan for AS/VIS was laid down, let alone produced specific requirements for subsystems such as vibration isolators. Therefore this report and the AS/VIS demonstration system itself should be viewed as showing what is possible rather than precisely what is needed. It can be said however that that AS/VIS has demonstrated the ability to exceed any likely ABL requirement for vibration isolation under nominal operating conditions. Further trade studies to be made during ABL development will determine how much of the demonstrated potential is needed and justified for application.

¹Presentation material for AS/VIS SBIR Phase II kickoff meeting, dated 17 February, 1994.

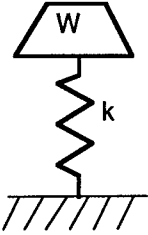
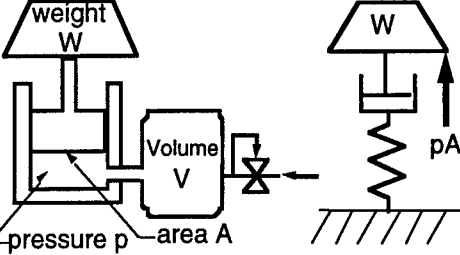
	Linear spring	Air spring
Model		
Deflection under payload weight	$W/K = \frac{g}{\omega_s^2}$	adjustable to zero
Corner frequency ω_s , rad/sec	$\sqrt{kg/W}$	$\sqrt{\frac{\gamma gA}{V}} \sqrt{1 + \frac{Ap_{atm}}{W}}$ $\gamma = \text{air constant}$

Figure 1: Pneumatic vs. linear elastic vibration mounts

1.1 Isolation for ABL Optical Benches

The vibration isolation problem for ABL has a number of special characteristics which are summarized in this section. Their effects on the design of AS/VIS will be apparent in later sections of this report.

The level of isolation required will be fairly high, on the order of typical passive laboratory systems currently in use, for example with research optical benches or electron microscopes. This implies a passive break frequency of a few Hz at most. Completely passive isolators such as metal springs or elastomeric "biscuits" will be inadequate, being limited by static sag to break frequencies no lower than about 5 Hz. This basic contradiction in requirements, low stiffness for isolation versus high stiffness to limit static deflection, can be resolved through the use of pneumatic mounts, or "airmounts". They have the very useful property that they are globally nonlinear but locally linear. That is, their small-displacement tangent stiffness, which controls isolation, is decoupled from global stiffness which determines static sag, such as caused by payload weight. Figure 1 illustrates this for the case of an ideal air spring where only the air contributes to stiffness.

Conventional airmounts are limited to minimum break frequencies of about 2 Hz. The bottom limit is set by the parasitic stiffness of the reinforced elastomeric bag or diaphragm used to contain the air. An important feature of the AS/VIS design is that it overcomes this barrier and has no minimum break frequency.

The choice of break frequency will be quite important. Unlike the laboratory environment where soft isolators are most often used, a 747 airplane is a large, flexible structure with numerous vibration modes below 10 Hz. A wing-bending mode,

for example, could easily put a large excitation component close to the suspension frequencies²; the isolator could actually make payload vibration worse. Such low frequency excitation must be handled either by (1) getting the passive break frequency very low, under the excitation frequency, or (2) actively stiffening the mount at low frequency while allowing faster than second-order roll-off to regain isolation at higher frequency, or (3) actively stabilizing the payload by using payload-mounted inertial sensors in feedback loops to tie it to inertial ground. AS/VIS is capable of implementing any of these strategies.

As usual in isolation problems, the high isolation provided by a low break frequency (soft mounts) brings with it an important limitation. Slowly varying loads will produce significant displacement of the payload. In the ABL case, such quasistatic loading will occur due to aircraft maneuvering. Local-vertical acceleration, normal to the aircraft floor, can exceed 0.2 g. With a 1.0-Hz suspension frequency, this translates to displacement of 1.95 inch (Figure 1). This may be unacceptable if the payload contains optics which must be held in registration to some off-bench datum.

Similarly, it is highly likely that several payloads (benches) will be used inside the ABL airplane, with various optical beams passing among them. This implies that at least the mean positions of the payloads must be held in registration to each other while individually they are still isolated from air frame vibrations. The need for soft suspension coupled with active mean-position control is clear.

Several aspects of the ABL isolation problem point to the need for an active system, or at least an active subsystem augmenting passive isolators. However most active isolators to date have been based on piezoelectric or magnetostrictive actuators. These are immediately ruled out for ABL because the spectrum of floor acceleration dictates much more stroke than can be provided by electrically induced material deformation. The latter are usually limited to, at most, a few mils of motion. Viable ABL isolators will require over an inch of stroke in each direction, and greater stroke would be a distinct advantage for risk reduction.

Finally, the ABL is intended to be eventually a front-line weapons system. This implies that all subsystems must be maintained and serviced under field conditions. Durability and ease of repair will be critical. As a laboratory demonstrator, AS/VIS has not yet attempted to meet this requirement. Rather, the objective at this stage is to identify the weak points with respect to ruggedness and maintainability and to assess the difficulty in "hardening" the system. Such attributes will become design requirements for actual flight versions to be developed by CSA under the ABL program.

²Suspension modes for an isolation system are those wherein the potential energy is confined to the isolation mounts themselves and the isolated payload moves as a rigid body. In classical isolation system analysis, the first few modes are always assumed to be suspension modes.

1.2 Technology Base

AS/VIS was not created entirely within this SBIR Phase II. Important elements are derived from CSA Engineering work on passive-active suspension systems for simulating zero gravity, much of it supported by Phillips Laboratory through prior SBIR projects. In particular, the very-low-frequency pneumatic mounts are based on hardware developed earlier. Figure 2 shows test data on a CSA suspension device. This proven capability for providing very soft, frictionless suspension was a primary motivation for the technical direction of the present project. Also shown is one of three large Gravity Offload devices built by CSA for the Phillips Laboratory for simulating zero-gravity with the 7200-lb SPICE structure. They demonstrated the scalability of the airmounts to a size well over that needed for AS/VIS.

The extensions required for AS/VIS concerned drastically increasing the active force capability, reducing the size and weight of the devices, providing integrated horizontal compliance and actuation, and developing control strategies for airborne use.

1.3 Summary of Accomplishments

AS/VIS has reached the stage of laboratory demonstration hardware. Figure 3 shows the system set up for vertical transmissibility testing. Summary descriptions of the various elements and their importance within the system are given below.

The system includes four passive-active isolation mounts, called airmount/actuators, which can jointly support payloads in excess of 3000 lbs. The entire vertical weight load is borne by a proprietary type of pneumatic mount with a second-order break frequency of 1.1 Hz. The pneumatic elements, essentially passive devices, can readily be changed without internal modifications to produce an arbitrarily low break frequency. Values of 0.1-0.2 Hz have been routinely demonstrated in other programs, including Phillips Laboratory SBIR projects ^{3 4}.

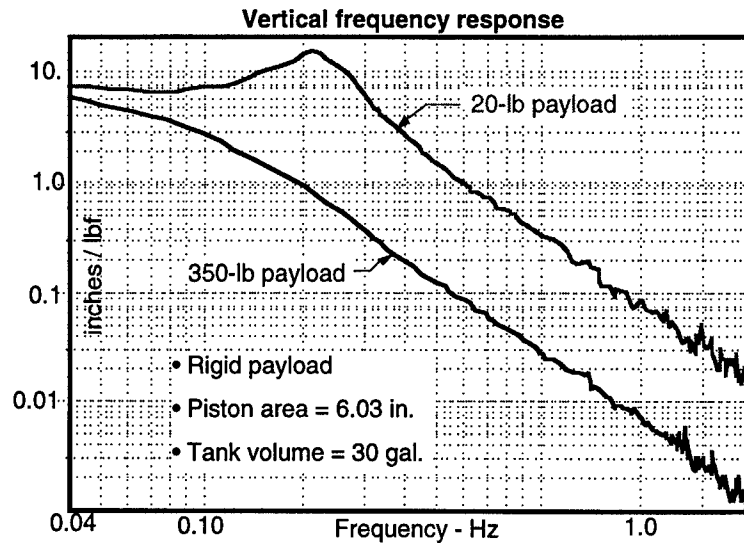
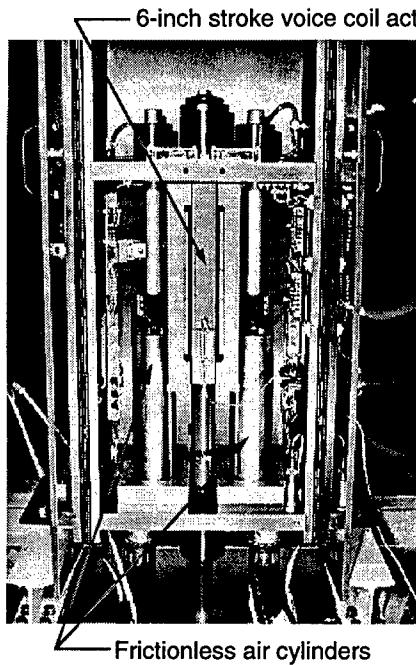
The airmounts use no elastomeric or other flexing elements to contain the compressed air. This allows them to circumvent the previous lower limit on break frequency. Vertical payload motion is accommodated with little or no friction through the use of air bearings at all sliding surfaces of the mounts.

The pneumatic mounts are used in series with an integrated passive flexure mechanism to allow horizontal suspension frequencies in the neighborhood of 0.75-2.00 Hz. A value of 1.26 Hz was demonstrated with a test payload of 1400 lb on four mounts. The flexures are essentially linear springs with highly predictable behavior.

³SBIR Phase II Report: Advanced Suspension System for Simulating On-Orbit Conditions, CSA Engineering Report No. 94-07-01, July, 1994

⁴Kienholz, D.A., "A Suspension System for Simulating Unconstrained Boundary Conditions," Proc. 12th Intl. Modal Analysis Conf., Feb. 1994.

Suspension device 60350-DA, one of five installed at NASA LaRC Large Structures Lab



2400-lb capacity, zero-G suspension device for SPICE

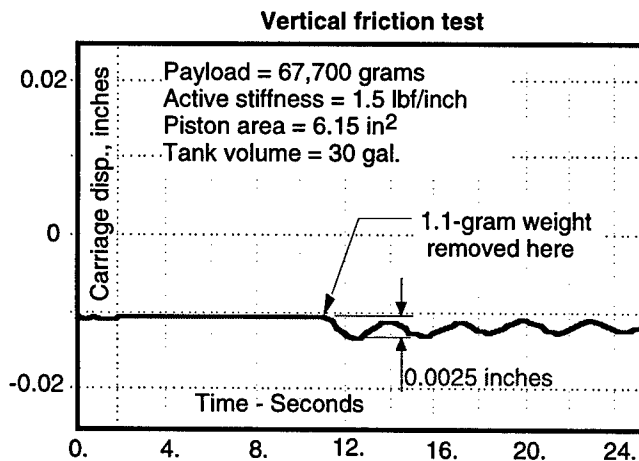
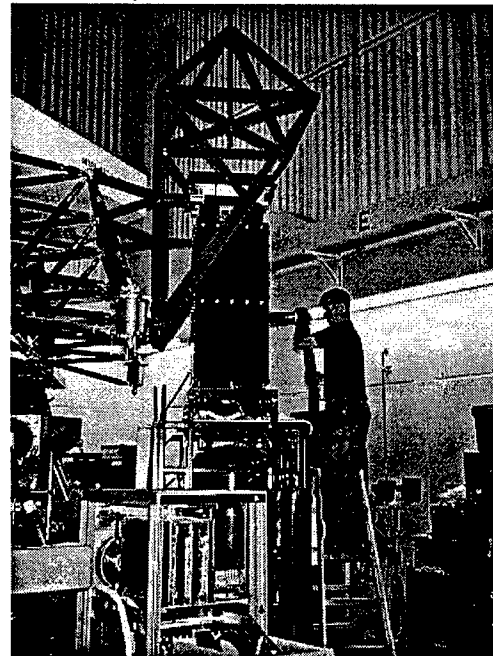


Figure 2: Pneumatic-magnetic suspension devices for zero-g simulation

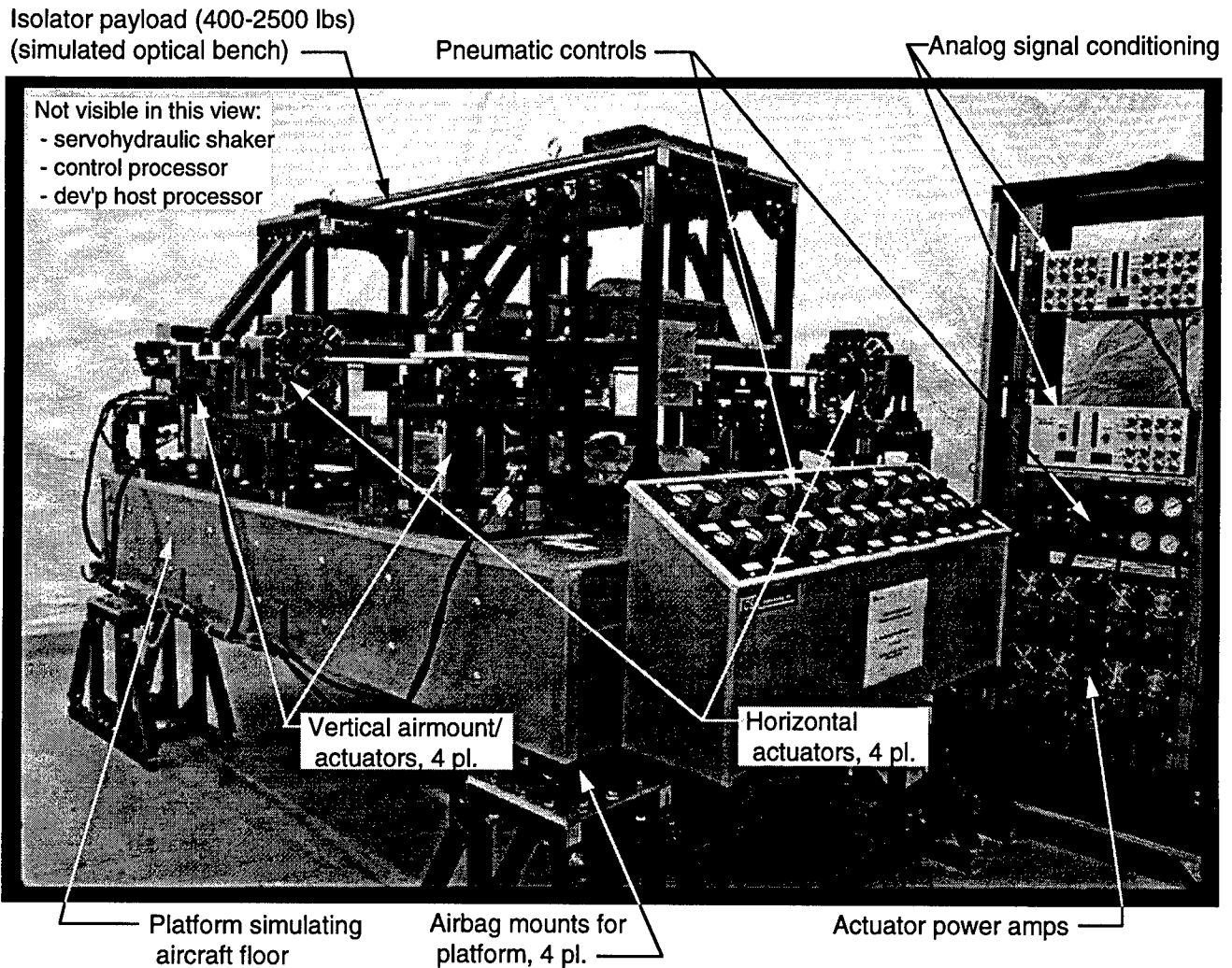


Figure 3: AS/VIS demonstration testbed. The entire system is sized for payloads heavier than the currently expected weights of the Airborne Laser optical benches.

The vertical mounts contain custom-designed integrated voice-coil actuators. Each can produce a force of about 220 lbs for about 10 seconds and about 180 lbs sustained. Four similar voice-coil actuators, separate from the vertical mounts, act on the payload, two in each horizontal direction. The actuators have a bandwidth in excess of 40 Hz. Thrust to weight ratio is in excess of 2.4:1, well above any commercial device having comparable stroke (1.25 inches vertical, 1.00 inches horizontal). Horizontal actuators also use air bearings to eliminate friction and stiffness between the moving element and the device frame. Horizontal and vertical actuators both include integral displacement sensors.

The high-force voice-coil actuators provide a variety of performance enhancements to the passive isolation system. Primarily, they allow control of the payload mean position in the presence of low-frequency quasistatic load variations due to aircraft maneuvering. They can also be used to slave the mean position of one bench relative to another, or multiple benches relative to some master reference. Using acceleration feedforward, they can offset such inertial loads without adding stiffness which would degrade isolation performance. They can be used with payload-mounted inertial sensors to actively stabilize the platforms in inertial space. The actuators can provide adaptive, on-the-fly stiffening of the system, either linear or nonlinear, for operation in turbulent flying conditions. They can provide active damping of suspension modes without degrading isolation at higher frequencies as passive dampers would. While not an objective of the SBIR, they may allow active suppression of low-order vibration modes of the optical benches. Such modes are usually the most damaging to aim-point beam jitter.

AS/VIS includes a real-time VMEbus control computer, 32-channel A/D and 8-channel D/A electronics, software development and operating system, and development host computer. A primary purpose of the demonstration system is investigating control laws and algorithms with realistic hardware-in-the-loop simulations. Baseline software for one particular control law has been developed for demonstration purposes and to shake out the entire system. Software has also been developed that allows the development host to be used as a real-time data monitor during operation.

AS/VIS includes extensive custom analog electronics for sensor signal conditioning and for driving the voice-coil actuators. The system includes 16 channels of DC-coupled accelerometer sensing with a bandwidth in excess of 340 Hz. Noise floor and sensitivity of the channels accommodate the range from the largest expected test input (floor vibration) to below the projected level on the isolated payload for moderate inputs. The DC-coupled acceleration sensing is also suitable for use with an acceleration feedforward control scheme.

Integrated signal conditioning is provided for eight displacement sensors, four each in the vertical and horizontal actuators. Resolution is about 0.0005 inches and bandwidth is over 200 Hz. Displacement signals are available both for diagnostic testing and for use in the control algorithm. Modular, current-drive linear power amplifiers and DC supplies are included, sized to drive the actuators to their thermal limits. In-

egrated preamplifiers are provided to match the D/A outputs to the power amplifier inputs. Patch paneling is provided to allow simple control laws to be implemented in analog for demonstration or diagnostic purposes.

The AS/VIS hardware (vertical airmount/actuators and horizontal actuators) has been integrated into a system-level test apparatus. It allows simulation in hardware of vibration of an aircraft floor. It includes a simulated optical bench as a test payload whose weight can be varied from 400 to about 2500 lbs. The acceleration sensors described earlier are mounted on the vibrating platform and the payload. Initial system-level tests have been performed to determine isolation performance in the vertical direction.

Initial full-up system tests have shown that passive, vertical-direction isolation in the 2-20 Hz range is essentially as predicted. Break frequency is 1.1 Hz with active stiffness set to its nominal value and 0.66 Hz with active stiffness off. Transmissibility crosses 0 dB at about 1.6 Hz and reaches -40 dB at 10 Hz. This performance is confirmed by component-level tests of single airmounts. Measurement of transmissibility at higher frequency is limited by payload dynamics and by acoustic shunt-path excitation around the isolators, just as it will be in actual ABL hardware.

In general, the AS/VIS system has performed as predicted and is now ready for its main purpose: serving as a proof-of-concept demonstrator and a development tool for flightworthy systems designed to actual ABL requirements. Numerous enhancements and improvements have been identified, both to the AS/VIS hardware itself and to the test apparatus.

2. Design Description

2.1 Concept and Operating Principle

The basic idea behind AS/VIS is quite simple. It consists of two essential elements.

1. The payload (optical bench) is "floated" with respect to the aircraft floor using very soft pneumatic mounts derived from CSA zero-G suspension devices as noted earlier. These can give a passive break frequency low enough to get under all important peaks in the floor vibration spectrum. Being virtually frictionless, they operate linearly over a wide range of input levels. They can give passive isolation substantially better than current-generation laboratory systems. Unlike current piezo-based active systems, they can accommodate over an inch of stroke, enough to be suitable for use in the relatively high-vibration airborne environment. However their extremely low stiffness will leave the payload vulnerable to large static displacements caused by changes in static loading such as due to aircraft maneuvering.
2. The payload is then coupled to ground by high-force voice coil actuators in all six degrees of freedom. The actuators are used to offset quasistatic force changes that would otherwise cause large rigid-body displacements of the payload on the soft mounts. In a sense, the actuators allow the active control system to "fly" the bench such that its mean position is slaved to that of the aircraft but the two are decoupled with respect to flexing motions of either. In straight, level flight, the active system can be used with payload-mounted inertial instruments to stabilize the payload in inertial space.

Figure 4 illustrates the concept. Three or more hard points on the payload are supported by airmount/actuators. Each spring is composed of a piston in a closely fitted cylinder connected by a large-diameter line to an external volume. From Figure 1, the dynamic stiffness (i.e. the suspension frequency) can be made very low by choice of the piston area and tank volume. The cylinder and external volume are pressurized by a precision regulator such that the pressure force just equals the part of the payload weight carried by that mount. The connection between each air spring and a payload hard point is through a flexure universal joint. This allows relative pitch and roll between the payload and mount. The cylinder body of each airmount (the part that does not move vertically with the payload) is fixed to ground through slender column flexures. The length and diameter of these flexures is chosen to set the horizontal stiffness (equal in both directions) such that the desired horizontal-mode break frequency is achieved. Since the flexures are loaded in compression by the payload weight, their stiffness is reduced by the negative differential stiffening effect⁵. This allows a very low horizontal break frequency to be obtained with prac-

⁵Young, W.C., *Roark's Formulas for Stress and Strain*, Sixth Ed., Table 10, Case 1b, McGraw-Hill, 1989

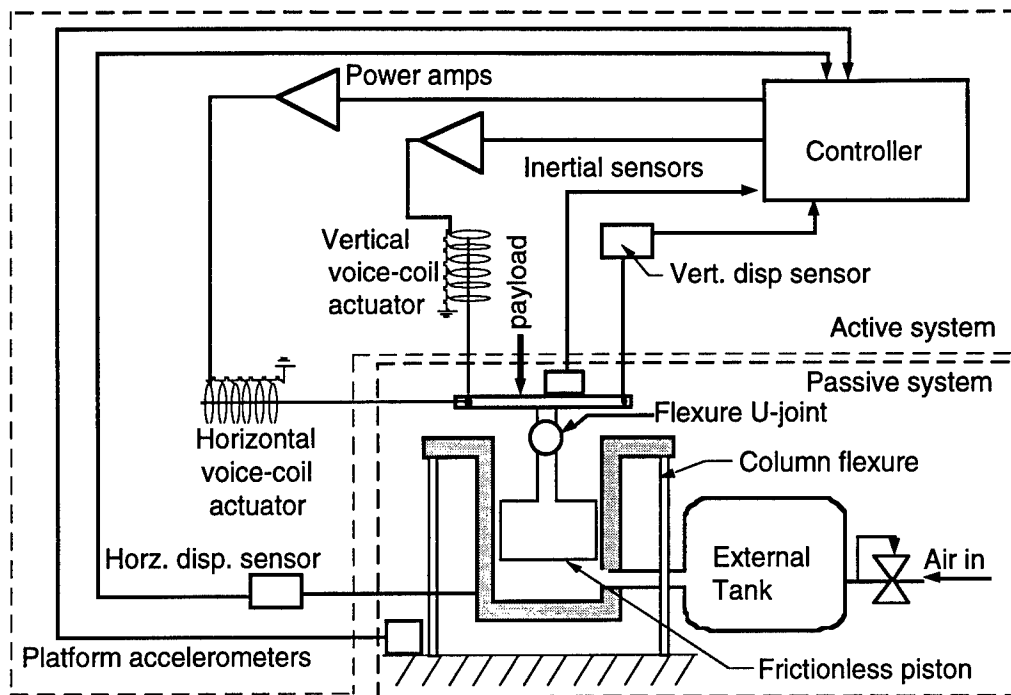


Figure 4: AS/VIS simplified operating principle

tical flexure sizes. The arrangement allows very low suspension frequencies for all six rigid-body modes of the payload on the mounts.

Horizontal and vertical voice-coil actuators act between the payload and ground. A minimum of six are required for rigid-body position control of the payload. The AS/VIS design uses eight with four acting vertically and two in each horizontal direction. Displacement sensors detect the position of each actuator moving element relative to ground. Accelerometers (DC-coupled) sense the low-frequency acceleration of the aircraft floor in inertial space. A minimum of six accelerometers are likewise needed. A controller implements some specified dynamic relationship between the sensed motion and the drive commands to each actuator.

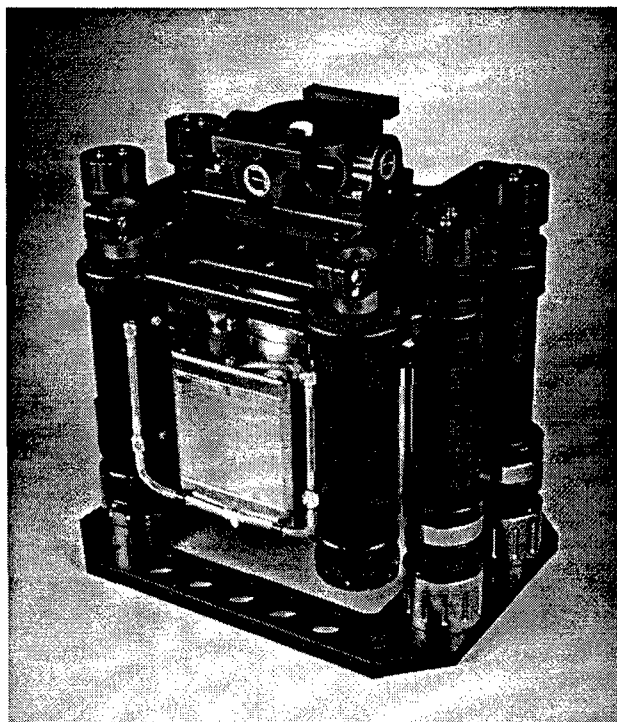
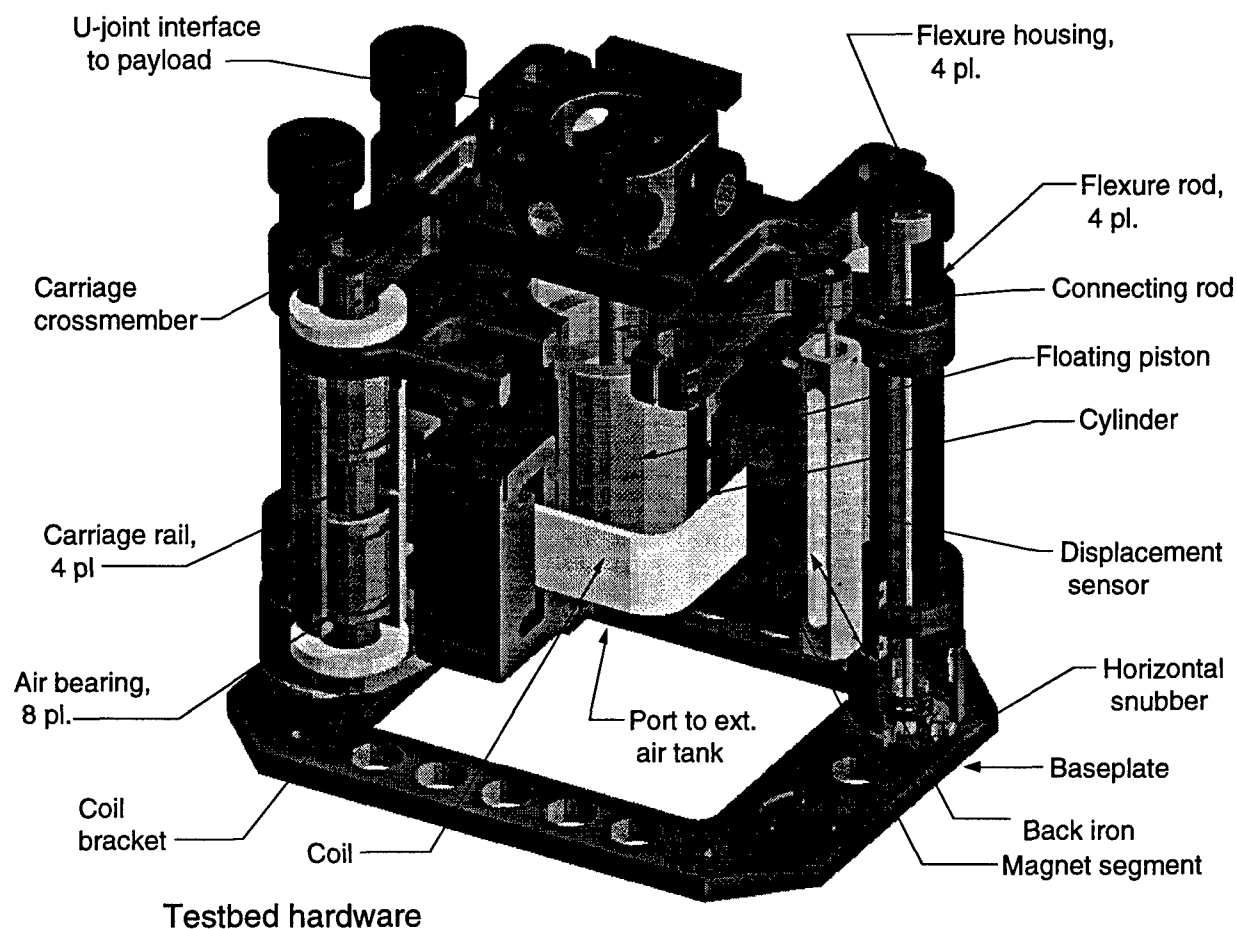
The engineering and design considerations required to realize this concept are described in the remainder of this section.

2.2 Vertical Airmount/Actuator

Figure 5 shows a cutaway view of a vertical airmount/actuator, a photo of one unit, and a table of nominal specifications. Figure 6 shows some subassemblies of the unit.

The vertical airmount consists of three main assemblies⁶: the baseplate which is fixed to the aircraft floor, the frame which is fixed vertically to the baseplate but moves horizontally on the four flexure rods, and the carriage which moves vertically on air bearings relative to the frame.

⁶These do not correspond exactly to the subassemblies shown in Figure 6



Nominal Specifications

Piston bore:	4.0 in.
Payload capacity (per mount) :	
at 30 psig	350 lbs.
at 100 psig	1230 lbs.
Vertical frequency (350-lb payload)	
active off, 2.0 gal. ext. vol.	0.66 Hz
active off, 10.0 gal ext. vol.	0.32 Hz
active on, 24 lbf/in, 2.0 gal ext. vol.	1.05 Hz
active on, 400 lbf/in, no ext. vol.	3.55 Hz
Horizontal frequency (350-lb payload)	
active off	1.26 Hz
active on (400 lbf/in)	3.10 Hz
Stroke (bumper to bumper)	
vertical	1.25 in.
horizontal	1.00 in.
Friction (% of payload):	< 0.01%
Actuator force constant	24.0 lbf/amp
Actuator force capacity	
intermittent	220 lbf
sustained	180 lbf
Weight	146 lbf

Figure 5: Vertical airmount with integral voice-coil actuator

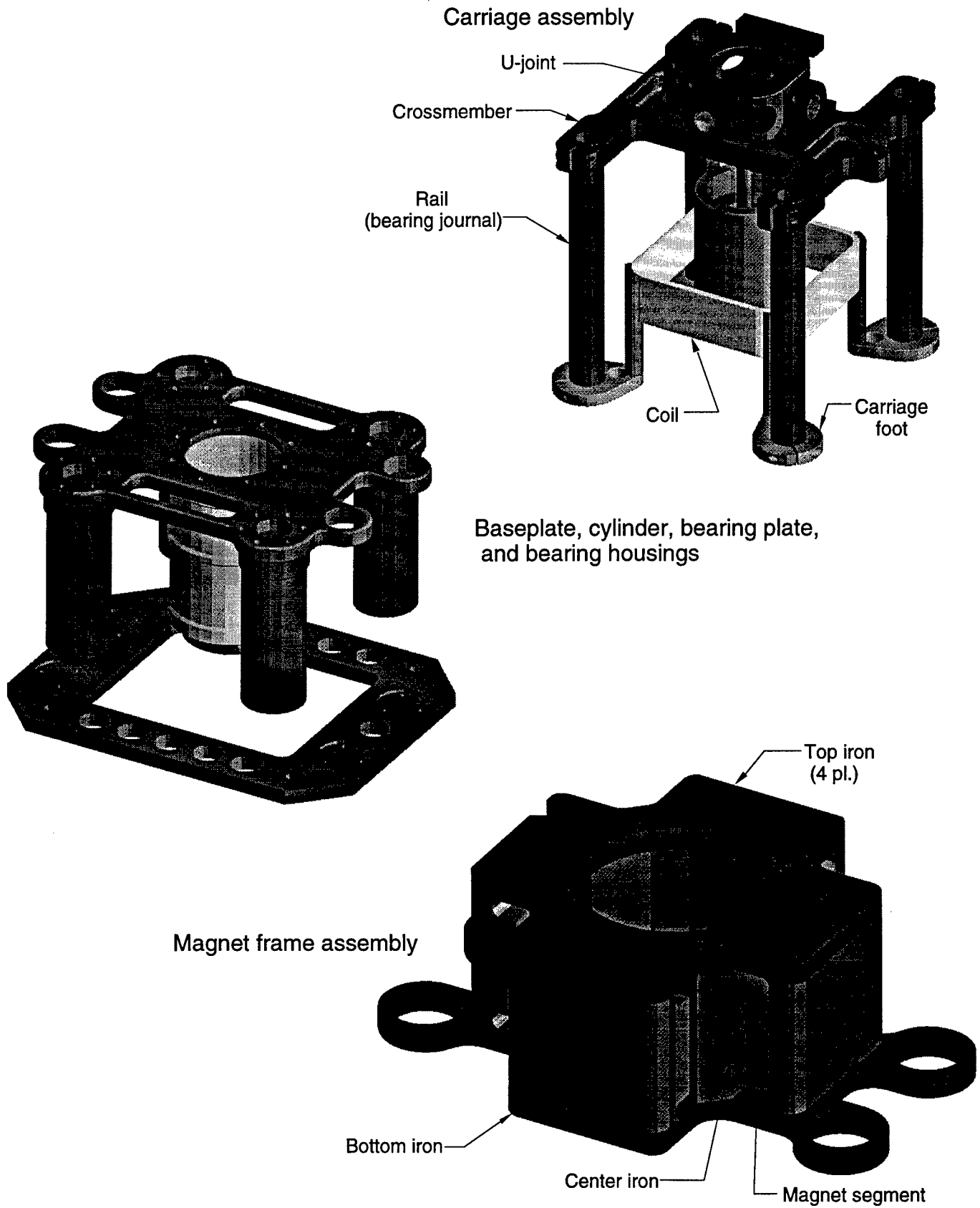


Figure 6: Vertical airmount subassemblies

The air cylinder is positioned at the center of the unit and serves as a primary structural member of the frame. At its upper end, it supports the bearing plate to which are fastened four cylindrical bearing housing tubes. These extend downwards from the bearing plate. Inside each housing are mounted two air journal bearings as shown. A total of eight air bearings are used per isolator.

The main parts of the carriage (see Figure 6, upper right) are a crossmember, four tubular rails which form the bearing journals, the air piston, a connecting rod, and a flexure U-joint assembly mounted to the top of the crossmember. The two upper trunnions of the U-joint assembly fasten to the payload. When air pressure is applied to the piston, it lifts the piston, carriage, U-joint, and one point of the payload. The U-joint allows pitch and roll of the payload relative to the air mount frame. The air bearings allow vertical motion of the payload relative to the airmount frame (and thus relative to the aircraft floor) and the flexure rods allow horizontal motion of the frame (and thus the payload) relative to the baseplate (and thus the aircraft floor). When the payload is mounted on several airmounts, the flexure rod action allows yawing motion of the payload, thus completing the six degree-of-freedom isolation mounting.

The piston is a proprietary frictionless design that uses special internal air circuitry to produce an air bearing film around its skirt. It does not actually touch the cylinder, but rather uses a small, controlled air leakage to produce the required lubricating film. Developed partially through prior SBIR support⁷, it is the key to obtaining high payload capacity, low stiffness, and zero friction. The lower end of the cylinder is connected via a 1.5-inch-diameter line to an external accumulator tank. The tank volume is 2.0 gallons for the demonstration testbed system. This was chosen to give a 0.66-Hz pneumatic suspension frequency when used with the 4.0-inch-bore piston supporting 380 lb. Connection to the tank is via a single line so a larger or smaller tank can easily be substituted to adjust the passive stiffness. The connection to the precision regulator feeding the air spring is made at the tank.

Voice coils are used for actuators because they can provide highly linear, long-stroke actuation with adequate bandwidth. High energy, rare earth magnets are used with air jet cooling of the coils to obtain a high thrust/weight ratio.

The vertical actuator coil is roughly square in plan view with rounded corners. It is positioned around the air cylinder for compactness. The magnet frame uses four magnet segments, one along each straight section of the coil. Magnetic design analysis of the actuator is covered in a later section of this report.

The wire size and number of turns in the coil are optimized to produce a good combination of coil resistance, inductance, and wire packing fraction. The "bottom iron" of the magnet frame (Figure 6, lower right) serves two purposes. It is part of the magnetic flux path and also serves as a primary structural member of the frame. The four "ears" protruding from the bottom iron (Figure 6) mount flexure housing tubes which extend upwards, fastening to the flexure rods at their upper ends.

⁷op cit "Advanced Suspension System..."

Cooling air jets for the coil are integrated into the center iron. A manifold distributes compressed air to a system of 24 jets, four at each corner of the center iron. The air is directed against the inside surface of the coil at each corner for cooling. Jet sizes and air pressure can be adjusted based on cooling requirements.

Elastomeric bumpers are provided as travel stops for motion of the payload in all three directions. Vertical bumpers are provided by annular open-cell foam pads mounted to the upper sides of the carriage feet (Figure 6) and to the upper sides of the bearing plate surrounding the carriage rails. Horizontal bump stops are O-rings which surround the lower end of the flexure rods and contact a cylindrical collar threaded onto the lower end of the flexure housing tubes. The snubbing collars can be lowered by rotating on their threads to lock the frame horizontally. They can likewise be raised to enable horizontal isolation. When raised, they limit horizontal motion to ± 0.5 inches before contact is made with the snubber O-rings.

A noncontacting LVDT displacement transducer senses the vertical position of the carriage relative to the frame (Figure 5). All electrical connections to the airmount pass through a single cable and connector.

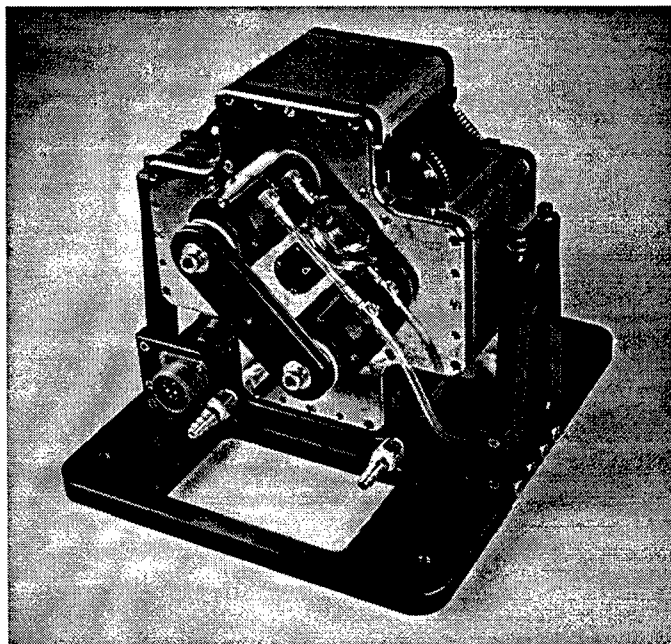
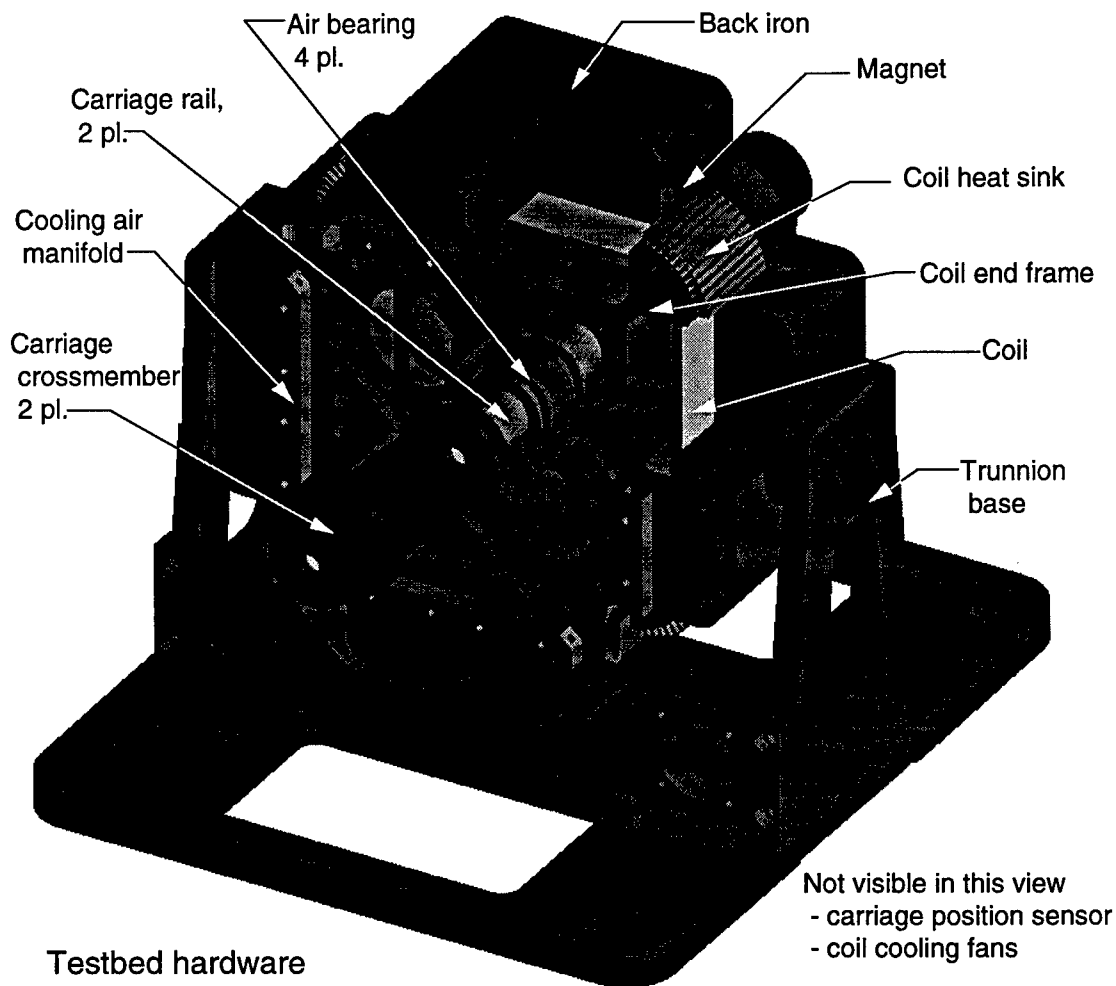
2.3 Horizontal Actuator

AS/VIS uses four horizontal voice coil actuators in addition to the four vertical actuators. The magnetic design of the horizontal units is very similar to the verticals. Magnet segments and coils are identical but back iron geometries differ slightly. The carriage assembly of the horizontal actuator is much lighter since it carries none of the payload weight. Figure 7 shows a cutaway view of a horizontal actuator, a photo of one of the demonstration units, and a table of nominal specifications.

Referring to Figure 7, the carriage uses two journal rails running in two air bearings apiece. The bearing housings mount to the end irons of the magnet assembly. The rails mount to the coil via lightweight aluminum end frames as shown. Two identical crossmembers tie the rails together at either end. A long pushrod, or stinger, transmits push-pull force from one crossmember to the payload. The pushrod uses ball joints at either end to avoid imposing moment on either the actuator carriage or the payload.

The only connection between the actuator carriage and frame is the two coil leads. The carriage runs on air bearings so there is no stiffness or friction force induced by carriage motion.

One end iron of the magnet assembly incorporates a compressed air manifold for coil cooling jets. These squirt air against the top edge of the coil along four sides, rather than against the inside corner surfaces as in the vertical actuators. In addition, the horizontals have two small axial-flow fans flushing ambient air through the coils from the inside out. The exposed corners of the coil mount finned aluminum heat sinks for additional cooling.



Nominal Specifications

Force capacity:	
intermittent	230 lbf
continuous	190 lbf
Force constant:	25.0 lbf/amp
Stroke (bumper to bumper)	1.1 in.
Bandwidth (3 dB)	> 40 Hz
Carriage suspension stiffness	zero
Carriage friction	zero
(air bearings used)	
Weight	96 lb

Figure 7: Horizontal voice-coil actuator

A noncontacting LVDT, identical to that in a vertical airmount, senses carriage position relative to the frame. The LVDT is positioned along the axis of the actuator and is not visible in the cutaway drawing. All electrical lines for the coil, fans, and LVDT run through a single connector on the base of the actuator.

The actuator body is carried in a trunnion mount which allows the elevation angle of the thrust axis to be easily adjusted. Weight of the trunnion base is included in the 96-lb figure given in the specification table. Thrust to weight ratio is over 2.4:1, about twice that of commercial electrodynamic shakers in this size range. This is obtained at the expense of bandwidth which is not needed in the present application. The relatively low frequency of the application is reflected in the fact that the coil is substantially heavier and has higher inductance than a commercial shaker of similar force rating.

2.4 Magnetic Actuators

This subsection describes the design of the voice-coil actuators used for both vertical and horizontal directions. Magnetically the two designs are very similar. They differ in that the vertical actuators are integrated with the air springs supporting the payload weight while the horizontals are stand-alone units which perform only the actuation function.

Each actuator is composed of two main elements: a wire coil and a magnet body. The two are designed such that the magnet body produces a flux field normal to the wire over most of the wire length. A current passed through the coil then produces a force normal to the flux and current directions (parallel to the coil axis). Figure 6 (upper right) shows the magnet body and coil separately for a vertical airmount. Force on a unit length of wire is the product of current and flux density. Maximum actuator force is determined by flux density in the coil, coercivity of the magnets (resistance to demagnetizing by the field from the coil), wire length in the flux, and maximum coil current. The latter is determined by heating of the coil.

Design of the actuator consists of determining a suitable arrangement of magnet, back iron, and coil. For AS/VIS, the design goal was to obtain a maximum force of at least 200 lbf with minimum weight. No hard maximum was set for weight but it was noted that commercial electrodynamic shakers of this size range typically have thrust/weight ratios of about 1.

It was obvious that the highest commercial grade of magnet material was appropriate. This was grade 35 (energy product of 35 million Gauss-Oersteds) at the time the magnet order was placed. However grade 40 magnets became available shortly thereafter at no increase in price so they were used.

Analytical design of the magnet body was performed using a 3-D boundary element magnetostatics code (AMPERES, from Integrated Engineering Software, Winnipeg, Manitoba, Canada). Input consists of a geometry description, B-H curves for

the magnet and back iron, and a specified number of amp-turns for the coil. Figure 8 gives material properties. Output is the flux field over the entire geometry and the net force on the coil. The flux field is then examined to locate areas of saturation in the back iron or low or uneven density in the coil. The back iron geometry is adjusted to eliminate such areas. Figure 9 shows a typical flux map. Such analyses were used to determine the force-current relation, the variation of force with coil position at constant current, and the coil inductance. The latter quantity is needed for designing the drive amplifier.

Certain practical constraints exist in design of the magnet assembly. Tensile strength of the magnet material is low which requires that it be well supported by the back iron and not used to carry structural loads other than the magnetic force. Magnet material is very hard and brittle and is consequently quite expensive to machine. Shapes of magnet material must therefore be kept simple. Rectangles are best for low-volume applications where special tooling costs must be minimized. Annular segments allow an annular coil where force is developed over the entire wire length. However this requires significant tooling investment. After considering a number of options, the designs shown in Figures 6 and 7 were chosen. They use a square plan-form coil with radiused corners. Magnets are rectangular slabs, magnetized through the thickness. Flux is imposed on the coil along all four straight sides with the corners used either for heat sinks (horizontal actuators) or as mounting points for the brackets that transmit the coil force to the carriage (vertical actuators).

Extensive analysis was performed in optimizing the coil and magnet geometry. For example, it was found that magnetic saturation was occurring in the back iron in areas where flux "turned the corner" as it entered the top and bottom iron. While some saturation is inevitable, it was found that soft iron fillets at the seams between magnet and back iron and between back irons and top/bottom iron could reduce saturation and improve coil force with negligible weight penalty. Such fillets were added to the design, either as integral parts of the machined back irons or as add-on pieces where necessary. The location of some of the fillets is visible in Figure 9.

Figure 10 shows calculated results for coil force at various coil positions along the nominal 1.0-inch stroke. The 200-lbf goal was met with some margin. As shown later, actual measured force is somewhat higher: 220-230 lbf. This is due primarily to the higher grade of magnets which became available after the analytical design was completed. The coil design was also improved slightly after these simulations were done.

The coil design is done concurrently with the magnet and amplifier design. It consists essentially of determining how many turns of what gauge wire should be used. More turns obviously mean more force per unit current. However as the wire gauge gets smaller, several limitations are encountered:

1. Coil resistance increases which means more heat per unit current. It also increases the required supply voltage for the amplifier and the maximum heat

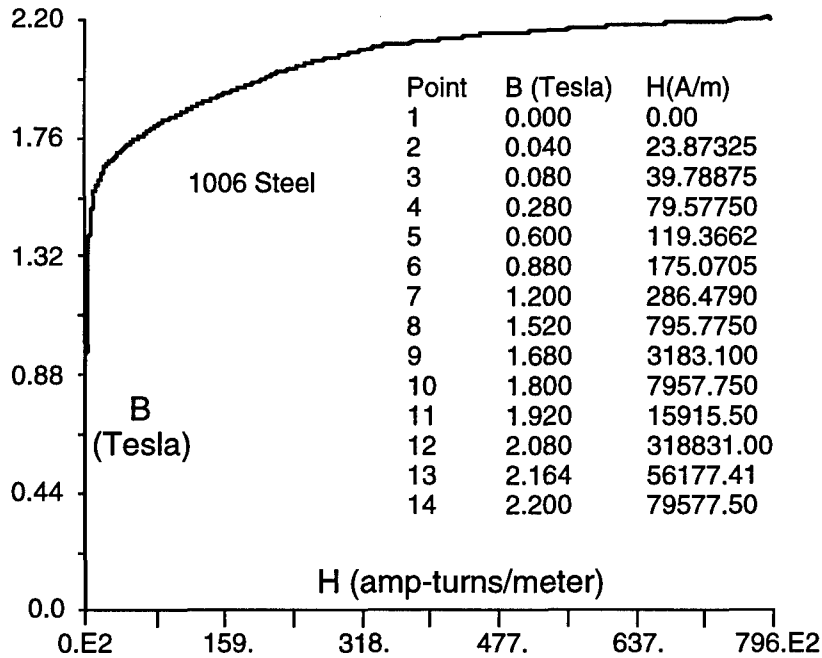
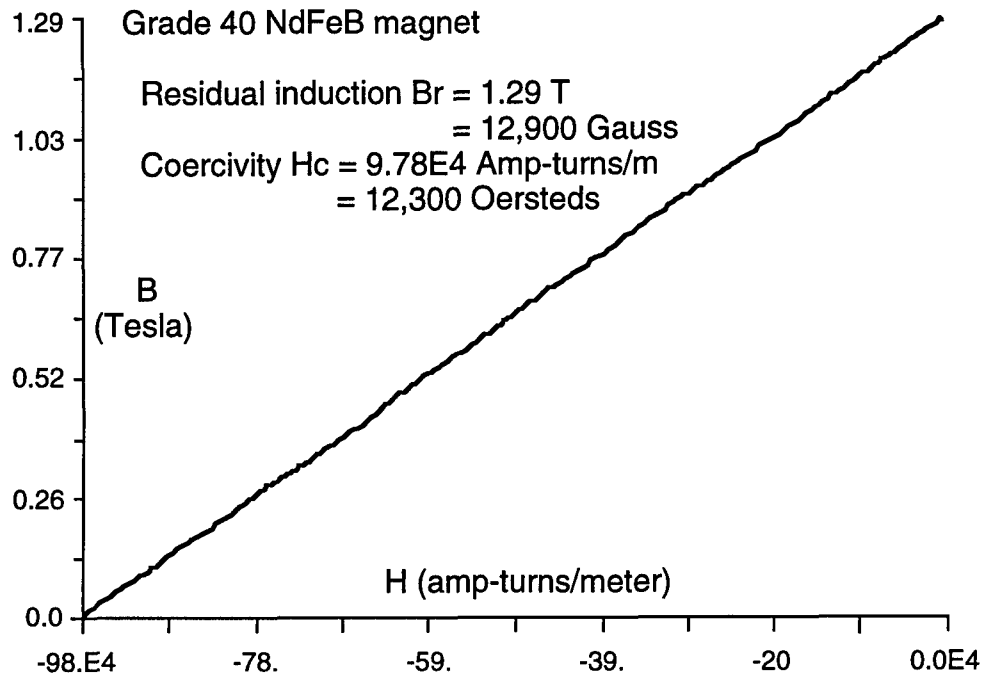


Figure 8: Demagnetization curve for magnet material (top) and BH curve for back-iron material (bottom)

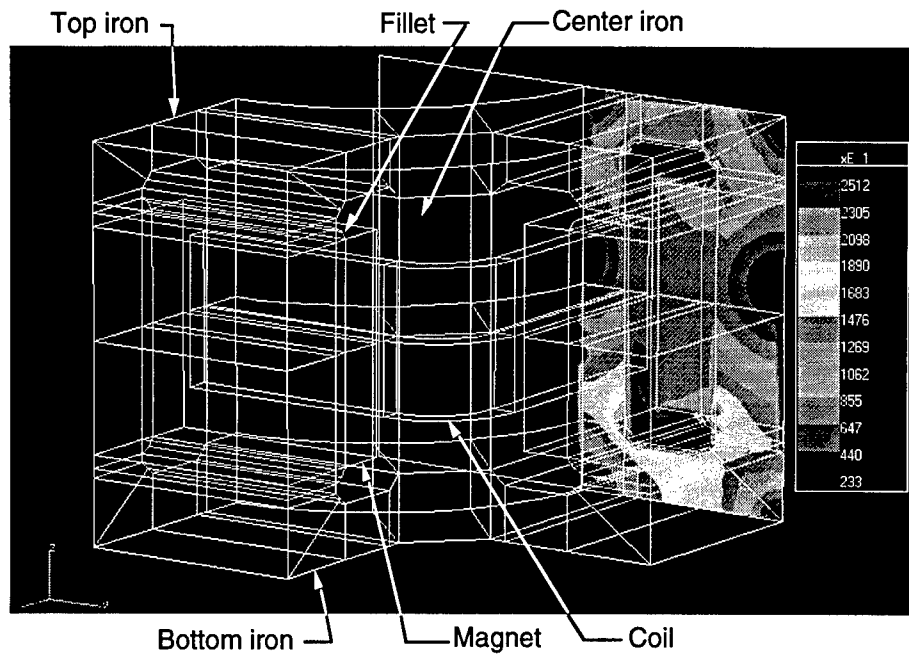


Figure 9: Calculated flux field at symmetry plane of voice coil actuator magnet assembly.

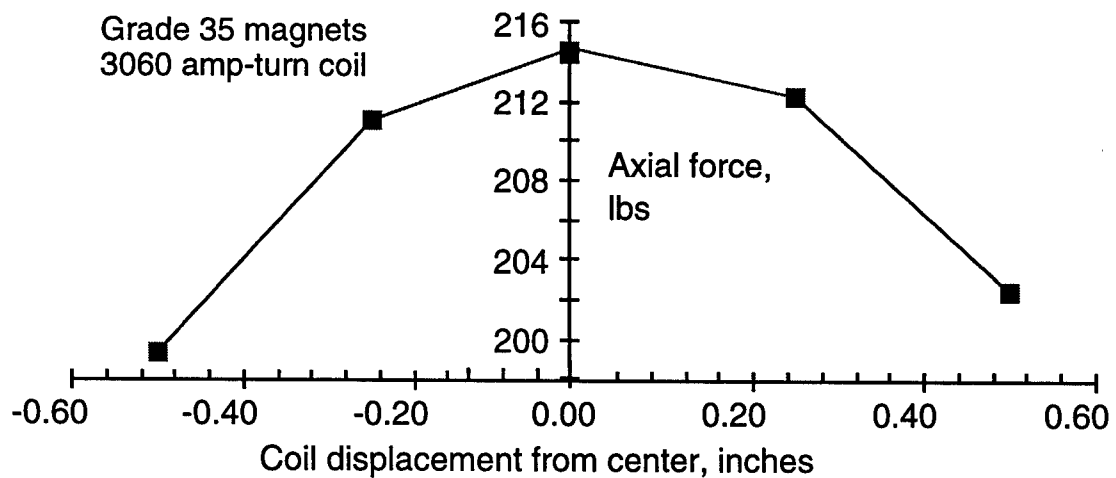


Figure 10: Calculated force vs. coil position for magnetic actuator.

dissipation for a linear amplifier.

2. Coil inductance increases which affects the required compensation for stabilizing the current-drive power amplifier.
3. A greater fraction of the coil volume is insulation and bonding agent rather than copper. This reduces the mechanical strength and heat dissipation capability of the coil.

The number of interacting variables and the relationships between them are sufficiently complex that no one-pass optimum solution is possible. However there is a simple practical approach that usually gives a workable solution. It uses the fact that there are only a fairly small number of wire gauges that are commercially available and physically suitable for coils of the required size. A spreadsheet was developed that calculated the parameters of interest (resistance, inductance, coil heating, amp heating, supply voltage, etc.) for all possible sizes. It was then a simple matter to scan through the possibilities, eliminate the impractical ones, and pick the best from the survivors. Figure 11 shows the resulting coil design.

2.5 Analog Electronics

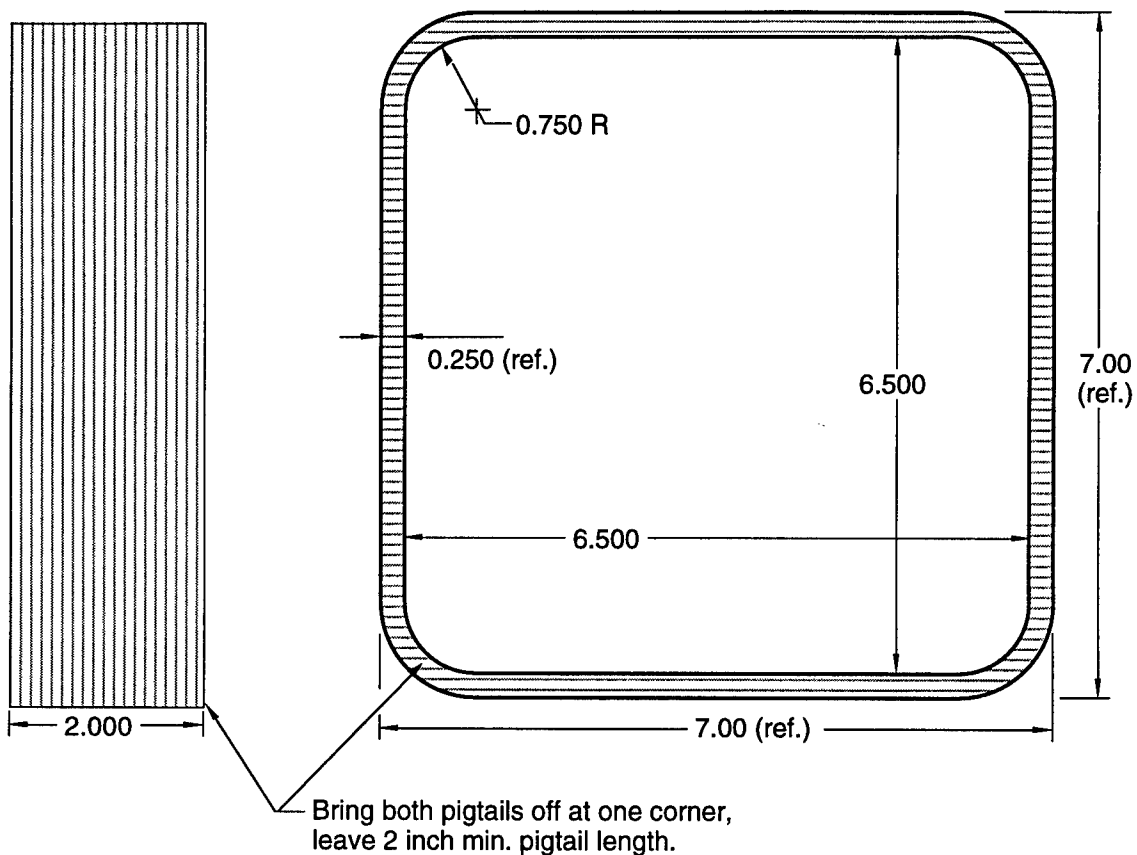
The AS/VIS testbed system includes extensive analog electronics, mostly custom but designed around off-the-shelf circuit boards and modules. As a testbed, the intent was to make the system flexible, easy to work with, and easy to maintain and repair if necessary. A design goal from the beginning was to make the system largely self-contained. That is, it was to have sufficient dedicated, built-in sensing and signal conditioning that both control law implementation and performance testing could be performed without temporary add-on equipment. Likewise it was desired that in situ calibration be possible for all signal chains.

This section describes the design and implementation of AS/VIS analog electronics. Detailed circuit diagrams have been supplied under separate cover as part of the final documentation package for the project.

2.5.1 Acceleration Sensing

A dedicated system of 16 acceleration sensing channels is provided. It uses a commercial instrumentation-grade sensor with integrated preamplifier and a custom chassis for gain scaling, DC offset nulling, and display. Primary requirements for the system were as follows.

- **DC coupling.** Acceleration sensing bandwidth must extend all the way down to zero frequency. This is necessary for implementation of an acceleration feed-forward control law as described in a later section.



Nominal coil specifications

Wire type: Copper, MWS, 18 AWG,
heavy-build insulation,
0.0431 dia., 6.386 ohms/k ft.

Layers: 6

Axial length = 2.00 inches

Wire termination: strip and tin

Pigtail length: 2.0 inch

Effective pitch = 0.0435

Turns per layer = 46

Total turns = 276

Outer perimeter = 26.28 in.

Inner perimeter = 24.71 in.

Surface area = 114.7 in²

Avg. length/turn = 25.49 in.

Total wire length = 7035. in.

Resistance = 3.744 ohms

Inductance = 234. mH (in magnet body)

Volume = 12.72 in³

Weight = 2.88 lbs

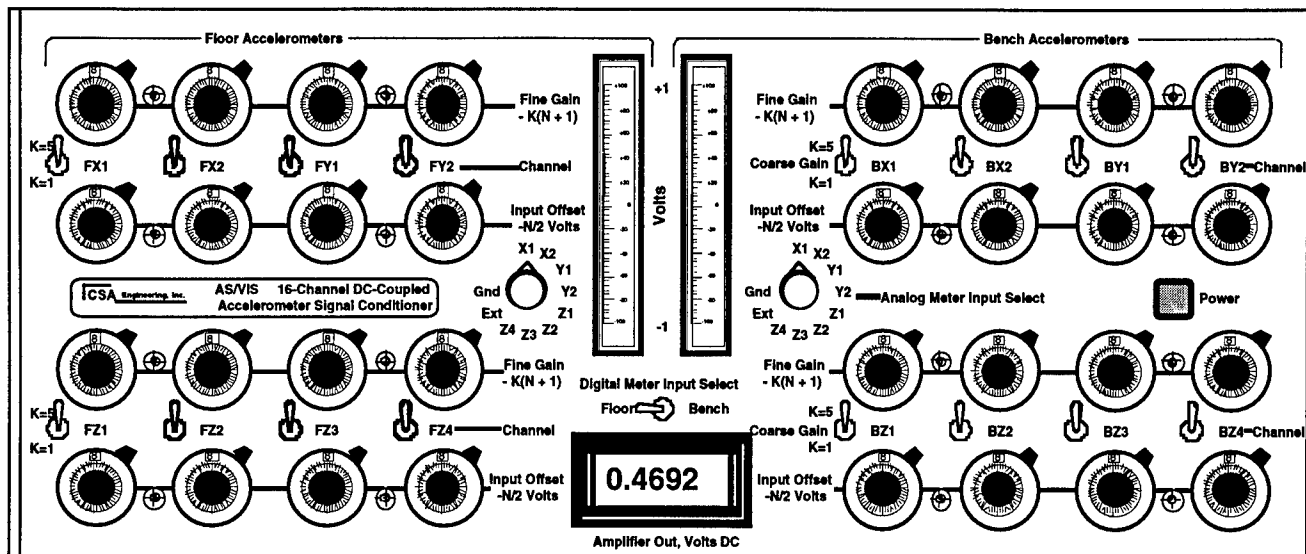
Figure 11: Actuator coil design. Some data are as-measured from prototype coil.

- **DC offset nulling.** DC-coupled accelerometers are always sensitive to their orientation relative to the gravity vector. A convenient means was needed for nulling out the DC signal present in channels sensing in other than the horizontal direction.
- **Bandwidth.** The system bandwidth had to extend past the frequency range where the isolator performance would be important. Nominally, this will be about 100 Hz in the actual airplane and about 30 Hz for the testbed. The latter figure is lower because the testbed payload will not have the high stiffness/mass ratio of an actual optical bench.
- **Channel count.** A sufficient number of accelerometer channels was needed such that all six rigid-body degrees of freedom could be transduced for both the isolated payload and the platform simulating the aircraft floor.
- **Rotational sensing.** Electronics were needed to allow differencing of three pairs of translational acceleration signals for the platform and three for the isolated payload.
- **Dynamic range.** The sensors and amps must be capable of measurements from below the expected level on the isolated payload to above the maximum level on the vibrating platform. Nominally these levels are 0.001 G and 0.5 G respectively.
- **EMI resistance.** The sensors had to be usable in the relatively poor EMI environment of CSA's laboratory. The building is near a Navy radio transmitter which often causes interference with measurement instrumentation.

Figure 12 shows the front and back panel of the chassis. It provides power, I/O connections, front-panel gain and offset controls, digital readouts for calibration, and fast analog bargraph readouts for signal monitoring during operation. Figure 13 shows a simplified diagram of one channel of the 16-channel system. Figure 14 shows accelerometer locations on the platform and payload.

The sensors are a piezoresistive type fabricated along with their preamplifiers on a single silicon chip (IC Sensors P/N 3140-002). They are DC-coupled with a nominal bandwidth of 0-340 Hz (+ 5% amplitude). Their manufacturer gives no noise floor specification but simple tests at CSA have indicated that it is less than 0.0001 G rms. Gain is variable at the chassis front panel from nominally 1.0 to 55.0 volts/G. The signal from the sensor is nominally 1.0 volts/G with a +2.5 Vdc offset. Sensor range is +/- 2.0 G, including the 1-G gravity field. The gain scaling amplifier can add an offset voltage from 0 to -5.0 Vdc to null the DC output. A sensor can be calibrated by detaching it from the structure (leaving the cable in place) and rotating it with respect to the gravity vector to produce a known 2.00-G change in the measurand input.

Front panel



Back panel

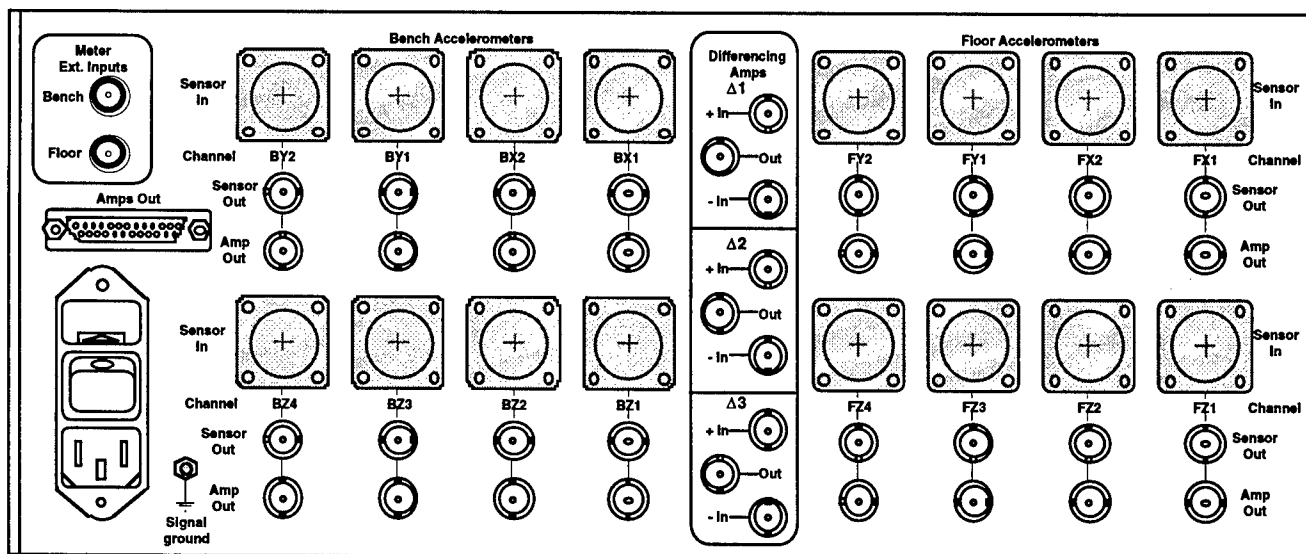


Figure 12: 16-channel accelerometer chassis.

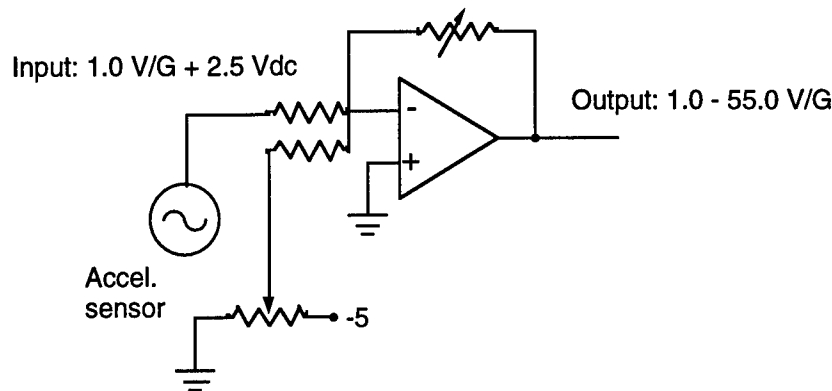


Figure 13: Accelerometer signal chain.

Gain scaling/offset amplifiers are housed in a single chassis along with three channels of differencing amplifiers. The latter can be patched via back-panel BNC jumpers to the outputs of the various acceleration channels to obtain rotational accelerations.

The accelerometers and amplifiers have performed well in testing of the AS/VIS. Their only serious drawback is that they use a type of connector not well suited for instrumentation. It is a five-pin, unshielded inline header designed to plug directly into a circuit board. For dynamic testing, they must mate to an in-line connector with an extension cable to reach the chassis. Cables with homemade connectors were devised for the laboratory system although a flight system will need a better solution.

2.5.2 Position Sensing

Relative position and orientation of the payload relative to the platform must be sensed. The likely usage of the displacement signals is in control laws, rather than performance testing of the AS/VIS. They could be used, for example, to implement local-loop uncompensated displacement feedback. The actuators would be used as simple linear or nonlinear springs for centering of the payload within its range of motion. Other more elaborate possibilities exist which are noted briefly in a later section on control laws.

Nominal requirements were set as follows.

- **Channel count.** A total of eight displacement channels was needed: one sensor in each vertical airmount and one in each horizontal actuator.
- **Resolution.** Position sensing accuracy of 0.001 was desired at each individual sensor. While somewhat arbitrary and probably more stringent than actually needed, this resolution was readily obtained and carried no real penalty.

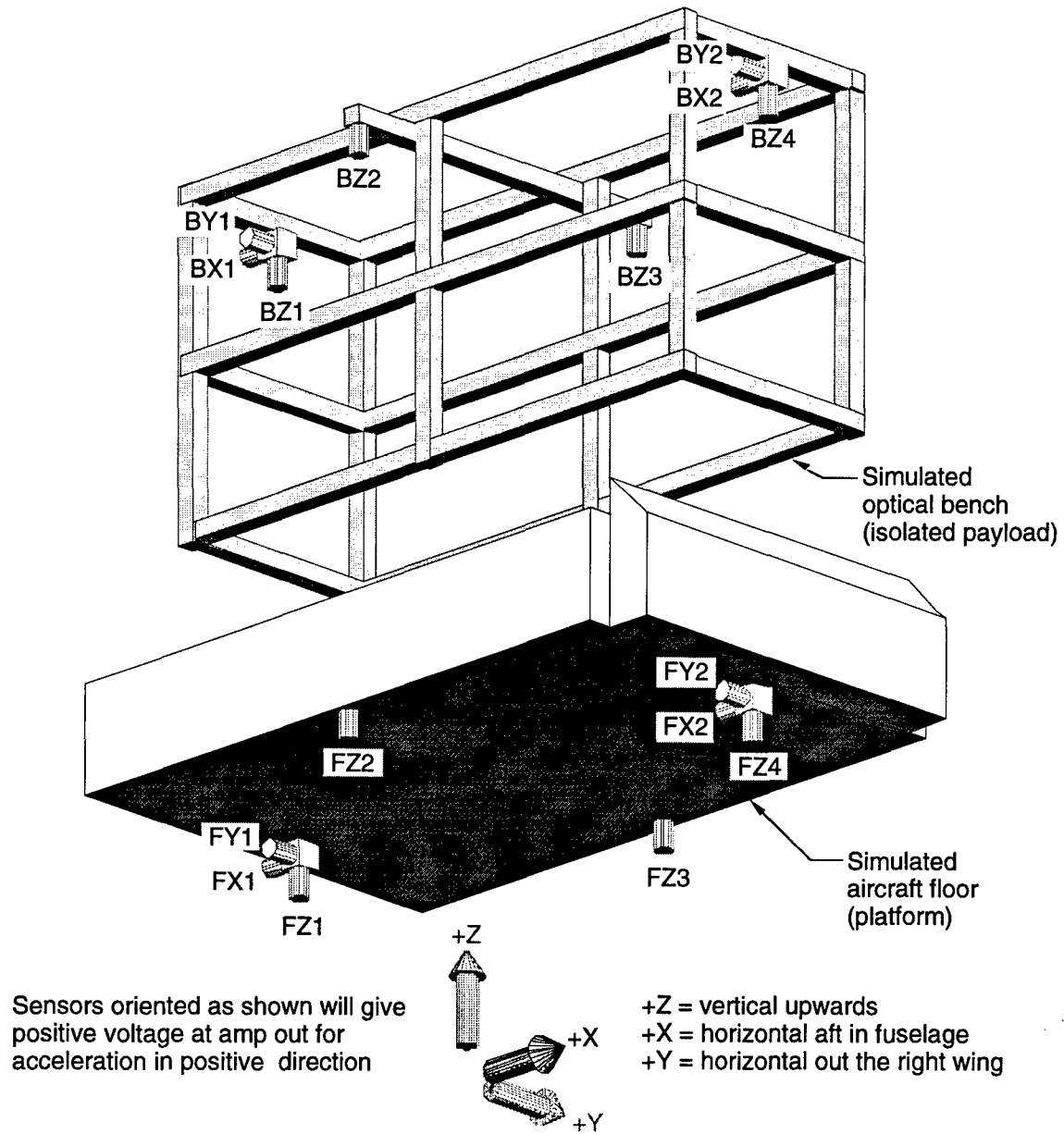


Figure 14: Accelerometer locations.

- **Bandwidth.** A 3 dB sensing bandwidth of 100 Hz was set. This was considered adequate to accommodate any control laws likely to be implemented in an actual ABL flight system.
- **Friction.** Since the airmounts and horizontal actuators are designed to be practically frictionless, the sensor had to be noncontacting.

Commercial linear variable differential transformers (LVDTs, Schaevitz P/N HR500) are used for position sensing. These are built into the actuators as described in Sections 2.2 and 2.3. Commercial board level amplifiers (Schaevitz P/N LVM110) are used in a custom chassis. Figure 15 shows the chassis. It provides power, I/O connections, and a digital readout for calibration. The chassis also contains eight preamplifiers for the actuator coil-drive amps which are described in a later section.

The range of motion and center position of each actuator are accurately known in advance. Therefore the desired zero and gain settings are fixed in advance and there is no need for front-panel controls. Calibration is done via trimpots on the individual amplifier boards inside the chassis. Gain of each is set at 10.0 volts per inch with zero volts corresponding to midstroke of the actuator. Nominal dynamic range of the sensors with their amps is over 60 dB, corresponding to a resolution of better than 0.0005 inches. Bandwidth is nominally 250 Hz (3 dB) and can be set wider by jumper changes on the board although this will tend to raise the noise floor.

2.5.3 Power Preamps and Amplifiers

Each voice-coil actuator has a discrete amplifier and preamplifier. Requirements for each channel of this eight-channel subsystem were as follows.

- **Current drive.** The power amplifiers had to be current drive, wherein the output current is proportional to the voltage input. This automatically compensates for changes in coil resistance due to temperature. It thereby stabilizes the relationship between actuator force and command voltage.
- **Capacity.** The power amplifier had to be capable of driving the actuator to at least 200 lbf. Based on the initial coil and magnet design, this translated to bipolar output of +/- 10 amps and +/- 38 volts.
- **Bandwidth** Like the displacement sensor, the amplifier had to have bandwidth adequate to accommodate the likely control laws and operating environment. Since both were undefined when the power amp was chosen, a design goal of 100 Hz (3 dB) was set although this was not a hard requirement.
- **Linearity and Distortion** It was decided that the power amplifier had to be of the linear type, as opposed to pulse width modulation. This was to minimize high frequency noise in the system which would work directly against the overall goal of vibration isolation.

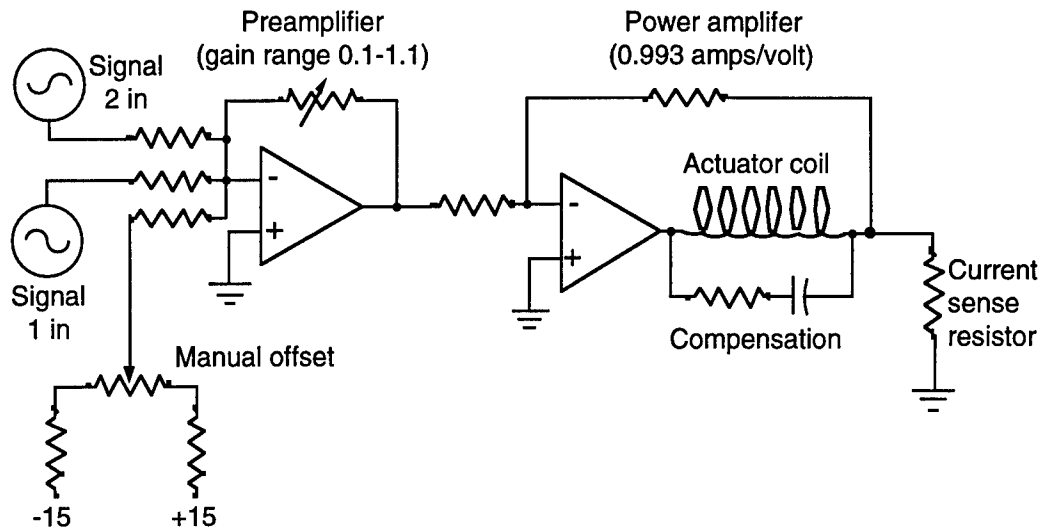


Figure 16: Power preamplifier and amplifier simplified schematic.

- **Analog gain and offset control** For flexibility in testing, it was desired to be able to close at least a simple displacement loop in analog with gain variable over about a factor of ten. A manual means for injecting a DC offset was also needed for testing and demonstrating the system.

Figure 16 shows a simplified diagram of the power preamplifier and amplifier for one of the eight actuators. The preamplifiers, housed in the chassis shown in Figure 15, are commercial, board-level operational amplifiers (Calex P/N MK155). They are used as single-ended, inverting preamps with gain controlled by a potentiometer in the feedback path. Gain range is 11:1. The preamp can also act as a summing amp with two inputs. One would normally be from the D/A converter of the control computer. The other can be from an external source if an actuator is to be used as a disturbance source for testing. It can also be from the LVDT output to close a simple displacement loop. This allows testing without the control computer and can, with some control laws, be used to reduce the CPU real-time computing load.

The power amplifiers (Inland P/N EM19) are linear H-bridge units which integrate the amplifier module, heat sink, and cooling fan into a single package. Figure 17 shows one module and the rackmount panel carrying all eight power amplifiers with their inhibit switches, pilot lights, I/O connectors, and other miscellaneous accessories.

Using the power amplifier (or any linear amplifier) in a current drive mode with an inductive load such as a voice coil requires compensation to stabilize the system. The compensation, shown in Figure 16, is a series combination of resistor and capacitor in parallel with the coil. In effect, this is a second feedback path which dominates over the first (the coil) at high frequencies where the primary path would induce too much phase lag and render the amplifier unstable. This circuit is slightly different from that usually used in current drive linear amplifiers. It allows the compensation

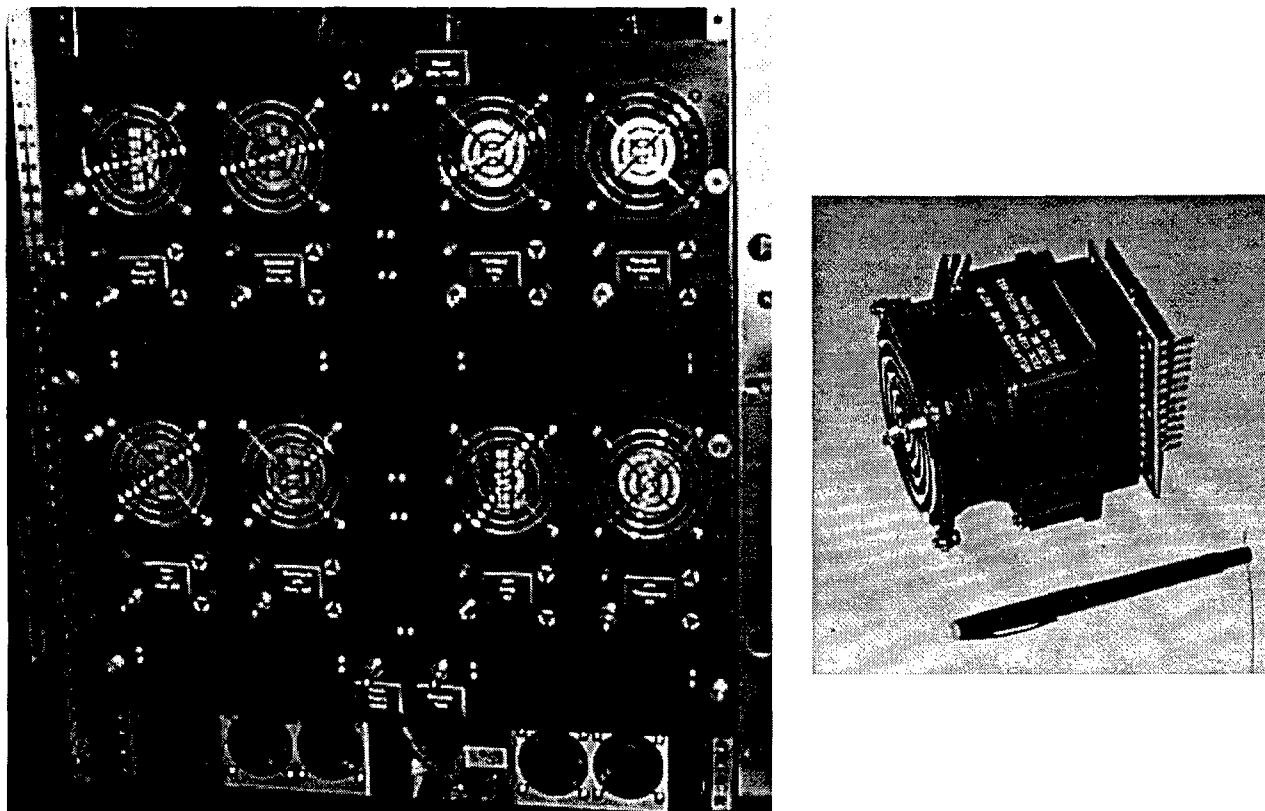


Figure 17: 8-channel power amplifier panel and amplifier module.

elements to be mounted at the actuator rather than at the amplifier, an arrangement that has packaging advantages in this application.

MatLab models of the actuator coil, power amplifier, and its compensation were developed for choosing the values of the compensator elements. Coil inductance was calculated by the magnetostatic model described earlier. Figure 18 shows the resulting closed-loop frequency response of the amplifier. While the 3 dB bandwidth is adequate at just under 100 Hz, it should be noted that the phase margin is not set at the bandedge. Rather it is set at lower frequency (in this case around 60 Hz) where the open-loop phase goes through a relative minimum.

2.6 Digital Control Hardware and Software

AS/VIS includes both a real-time control processor and a development host. Requirements, in some cases qualitative or simply design goals, were set as follows.

- **Flexibility** A primary purpose of the entire AS/VIS testbed is development of vibration control algorithms using advanced passive/active hardware. For effectiveness in this role, it was decided that a general-purpose real time processor and industry-standard bus architecture would be used. Likewise, it was highly desirable that the processor could be replaced by a later generation unit when

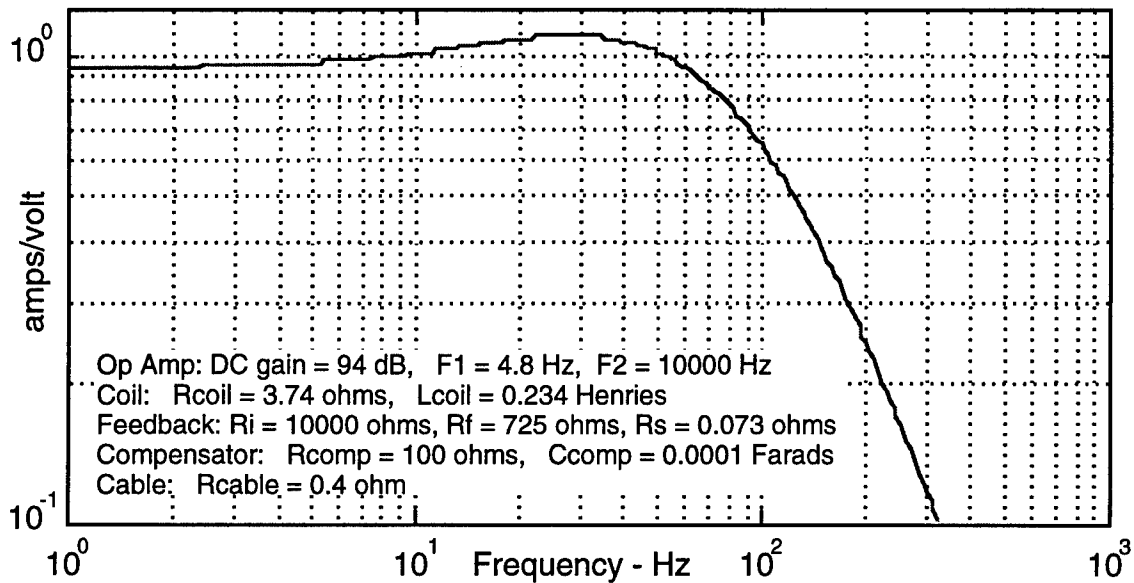


Figure 18: Frequency response of current-drive power amplifier.

such became available. A goal was to have processing done by a general purpose CPU rather than a specialized array processor or DSP chip. This would sacrifice some ultimate speed in favor of flexibility.

- **Traceability to flight systems** It was necessary that flight versions be derivable from the AS/VIS real-time system without extensive reworking of software. This again implies using a bus architecture and processor suitable for flight, even if the testbed AS/VIS system as a whole is not.
- **Computing speed** Computing power requirements were virtually impossible to estimate at the time a decision was needed regarding the real-time control processor. However since this processor is not itself a major cost item, it was decided to allow a substantial margin against the estimated requirements. The latter were not severe since the bandwidth of the control system need be only a decade or so greater than the suspension mode frequencies. The nature of the isolation problem itself guarantees that suspension frequencies would be a few Hz at most. After discussing the application with a number of manufacturers, it was estimated that a processor with a SPECfp rating of 15-20 or better would be adequate. Since actual throughput depends on many factor not measured by the SPECfp or SPECint ratings, a generous margin above this estimate was highly desirable. As a benchmark, the application is considered less demanding computationally than an industrial robot having a similar number of I/O channels.

- **Channel count** Based on the number of accelerometers (16) and displacement sensors (8), at least 24 A/D channels were needed and more were highly desirable to allow for future growth. Likewise at least 8 D/A channels were needed.
- **A/D and D/A speed** Because the analog data bandwidths are quite small, it was desired to avoid entirely the need for sharp anti-aliasing filters by using a high oversampling rate. A design goal of 1000 SPS was set for the A/D and D/A subsystems.
- **Software development efficiency** The purpose of AS/VIS dictates that it utilize state-of-the-art software development tools. While no attempt was made to set quantitative measures for efficiency, it was clear from the beginning that the variable cost of labor for custom software development would dominate over the fixed cost of even the most elaborate development system. Priority was therefore given to providing a complete, well-proven, well-supported software development environment.

A block diagram of the system hardware is shown in Figure 19. It uses a VMEbus for the real-time processor and its peripherals. This industry-standard architecture is widely used in industrial automation and is well suited as the basis for flight systems. Board-level processors and peripherals of all types are available from dozens of manufacturers.

The processor is a Heurikon/MIPS V3500 rated at 31 SPECfp and 33 SPECint. It has proven more than adequate for running the control algorithms developed within this project. It was considered quite fast when it was acquired in 1994 but has since been superseded. As a VMEbus board based on a MIPS chip, it could be replaced quite easily with a faster, more recent version if desired⁸.

The analog interface is provided by a 32-channel A/D and 8 channel D/A on a single VMEbus board (Pentland MPV956). The combination of processor and analog board has proven capable of 1000 SPS in true, deterministic real-time control using the control law described in Section 4.1.

The development host computer is a Silicon Graphics Indy workstation built into a common chassis with the VMEbus system. Data transfer between the two is via a bus-to-bus interface (Bit3 P/N 607). This fast interface allows the host computer to be used with a graphical interface for real-time data monitoring during operation.

The software development system and real-time kernel are VxWorks from Wind River Systems. This development environment provides a large variety of software tools and debugging aids. While relatively expensive, it is widely used, well supported, and features a stable, reliable real-time kernel.

⁸The logical replacement at present is a Heurikon processor based on the MIPS R4700 chip which is 2-3 time faster and uses less power.

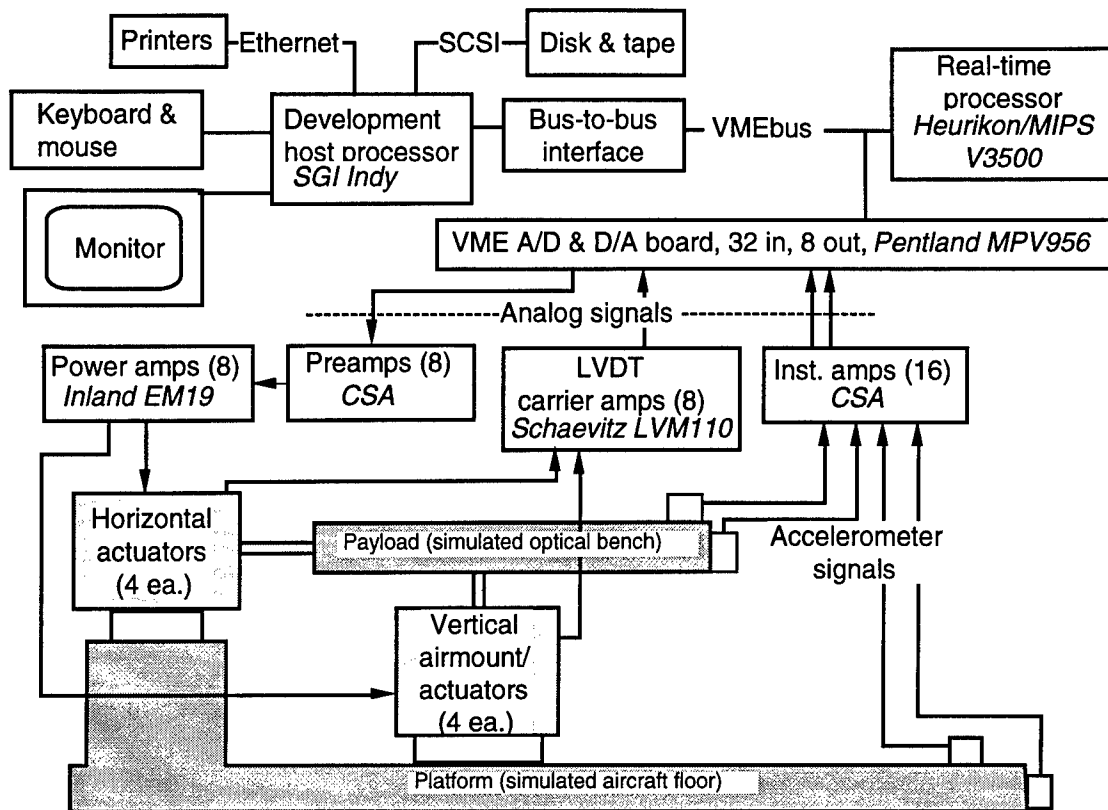


Figure 19: Block diagram of real-time control processor and development system.

3. Test Methods and Results

Preliminary testing has been completed on the AS/VIS demonstrator system. While this has been limited to laboratory tests (the entire system cannot be tested in an airplane for obvious cost reasons), certain important design goals have been verified. This section describes the methods, results, and conclusions of the tests.

3.1 Actuator Tests

The horizontal actuators have been tested to verify force capacity, force/current ratio, and frequency response. Figure 20 shows the test setup. The actuator trunnion is fixed to a rigid base and the carriage is fixed to a rigid bookend fixture through a load cell. A DC or random voltage signal is applied to the actuator preamplifier and the resulting force from the actuator is sensed by the load cell. For static measurements, voltage input to the preamp and output from the load cell are measured point by point with a digital voltmeter. For dynamic measurements using random input, the output and input voltages are applied to the numerator and denominator channels respectively of a digital Fourier analyzer and the frequency response is measured. Coil temperature was also measured during static tests by means of a noncontact infrared thermometer.

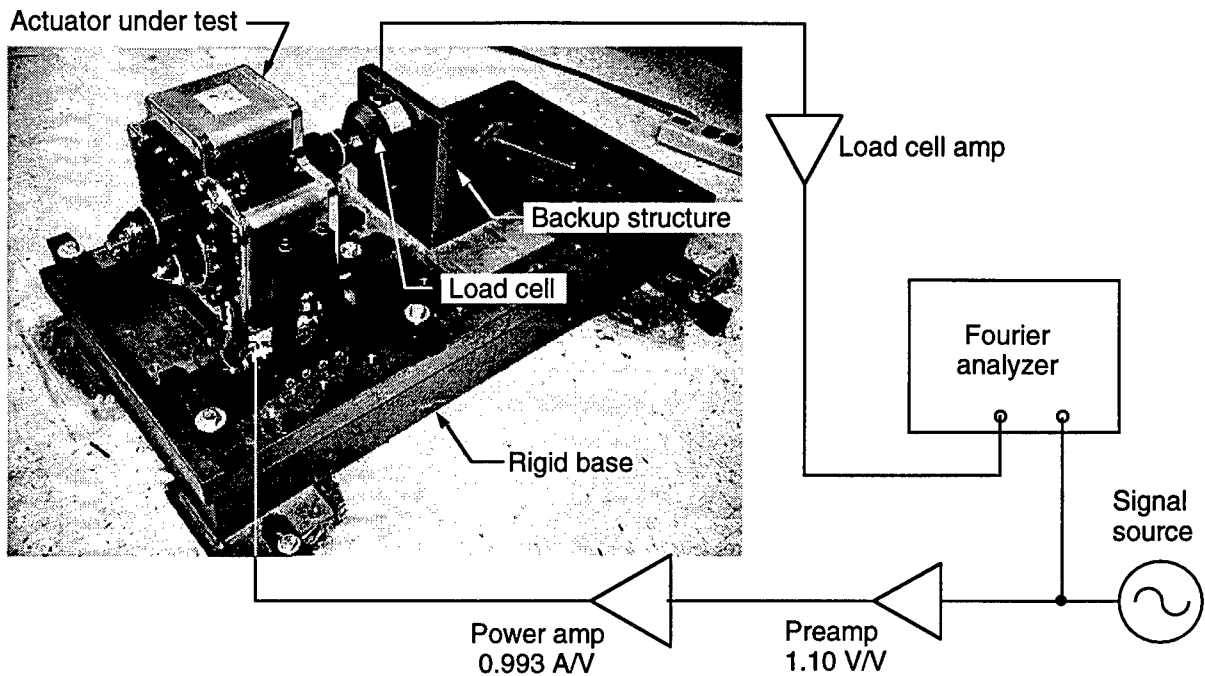


Figure 20: Testing of horizontal actuator.

In addition to dynamic tests described later, vertical actuators were tested statically by operating them against a constant force developed by the air piston. This constant force was determined by measuring the piston air pressure with a mechanical gauge and using the known piston area to calculate force.

Static testing of horizontal actuators established that coil cooling is quite adequate, at least at sea level. Coil temperature never exceeded 200 degrees F under continuous full load using only the cooling fans. The compressed air cooling jets were found to be unnecessary. The manufacturer of the coils rates them conservatively for a maximum temperature of 302 degrees F although a nominal design maximum of 250 F was set for this application. Running the coils too hot causes heating of the magnets which reduces actuator force/current ratio. While the effect is reversible, it is undesirable from a control standpoint.

Coil cooling of the vertical actuators needs further development. They were found to reach 180 F at a current of 5.7 amps continuous with 40 psig on the cooling jets. This extrapolates to 250 F at 7.2 amps, well short of the desired full load value of 10.0 amps. The solution may be nothing more than increasing the size of the cooling jets or increasing the air pressure. This was not done during these initial tests for reasons of schedule. Ideally, fan cooling would be used on flight versions of the vertical actuators as well as the horizontals. This will be investigated during design of flight versions of the AS/VIS for the ABL program.

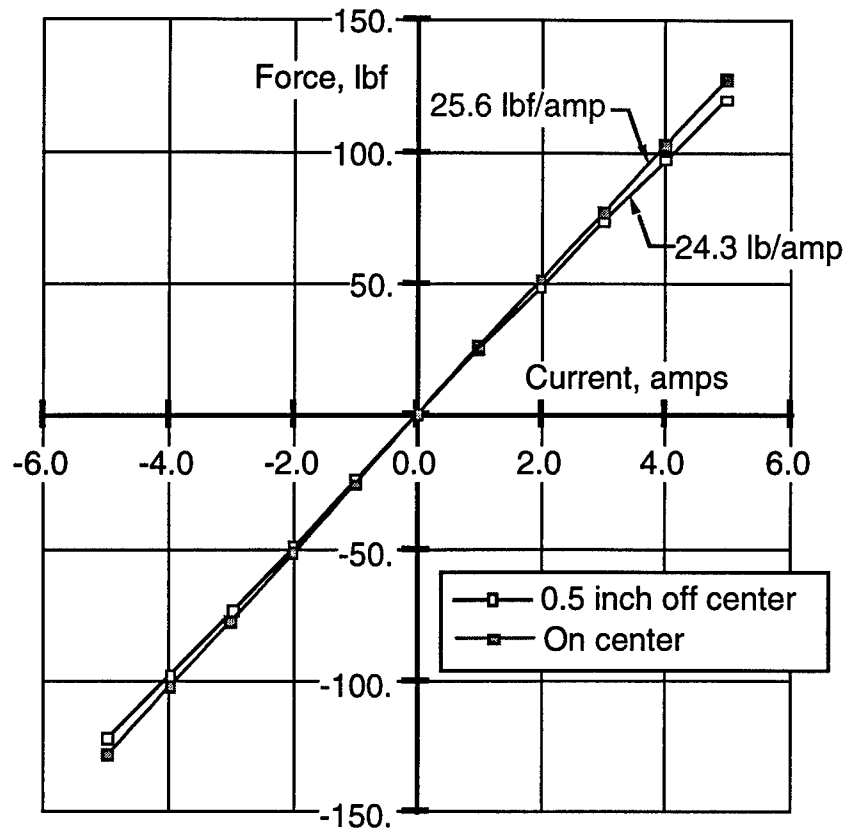


Figure 21: Static test results for horizontal actuator.

Maximum force capacity was of secondary interest at this stage because it could not be utilized during system-level laboratory tests anyway. Even at maximum displacement loop gain and maximum safe level of vibration input, the actuators are utilizing only a fraction of their force capacity. The real importance of actuator force capacity is in airborne operation where steady G loads must be offset for periods of several minutes.

Figure 21 shows static test results for a horizontal actuator. Force/current ratio was found to be nominally 25.6 lbf/amp with the coil centered in its stroke and slightly less near the ends. Force is highly linear with respect to current at a fixed coil location. Static tests of a vertical actuator gave a slightly lower value, nominally 24 lbf/amp. A slight nonlinearity between force and current was noted near full load but the horizontal actuators were found to give 232 lbf output at 10 amps. This is well over the target of 200 lbf and was quite satisfactory.

Figure 22 shows the results of blocked-force frequency response testing of a horizontal actuator. Some mild dynamics is evident in the low frequency range below about 20 Hz. This is still unexplained but the cause is suspected to be amplifier-load dynamics and/or eddy current losses in the actuator back irons. It will need further investigation prior to using the actuators in a flight system since it could complicate system-level control behavior.

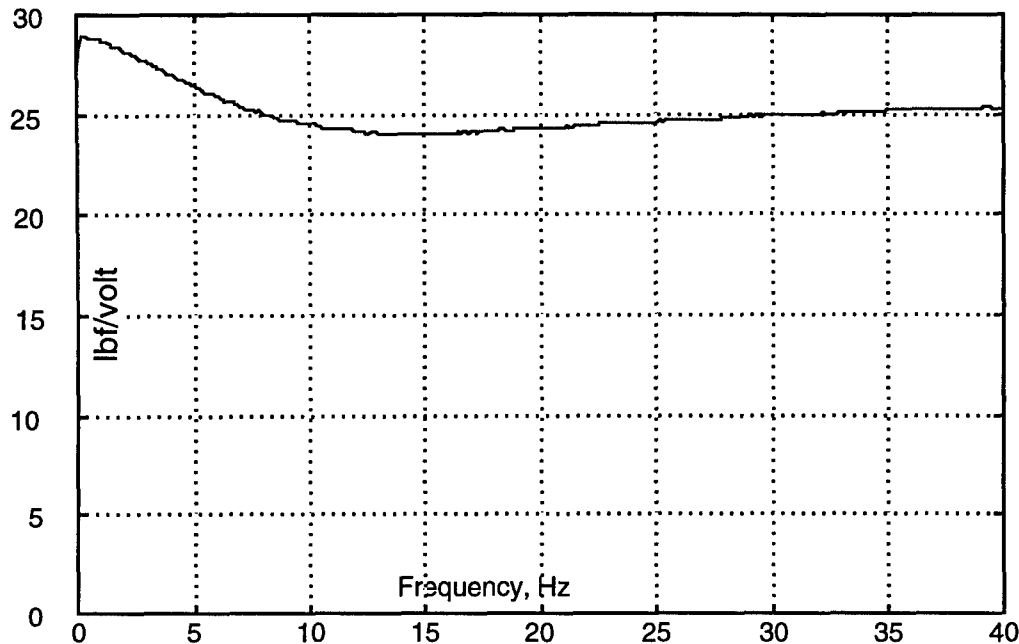


Figure 22: Dynamic test results for horizontal actuator.

3.2 System Test Apparatus

An apparatus was designed and built to allow testing of AS/VIS at the full system level with four vertical airmounts and four horizontal actuators. Illustrated in Figures 3 and 23, it is essentially a vibrating platform to simulate the aircraft floor in flight and a payload structure simulating an optical bench. The latter is supported on the former by the four AS/VIS vertical mounts. The four horizontal actuators mount to the platform and act against the isolated payload, two in each horizontal direction.

The platform and payload are both constructed of Unistrut and plywood with custom machined parts only for interfaces to the isolators, actuators, shaker, and soft mounts under the platform. The platform has an internal Unistrut skeleton with plywood skins all around to increase bending and torsional stiffness. The payload is a Unistrut frame with three plywood decks. Bags of lead shot and lead bricks are placed on the payload decks to obtain the desired weight and C.G. location. A typical test configuration (Figure 3) has the payload loaded to a total weight of about 1400 lb with its C.G. slightly below the plane formed by the interfaces to the vertical airmounts.

The platform is supported off the lab floor by pedestals and air bag springs as shown. This gives a fairly low mounting stiffness which allows the platform to be

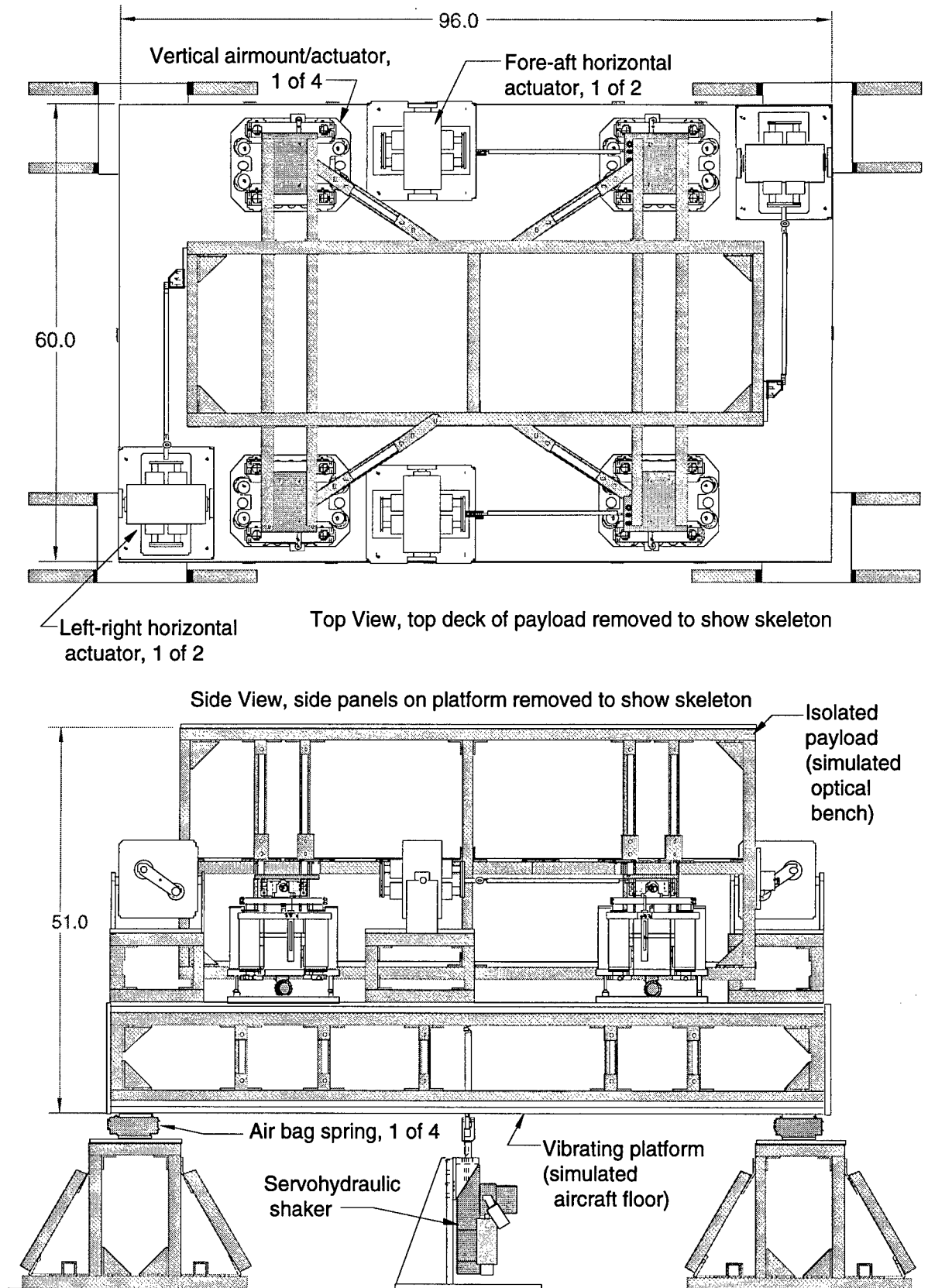


Figure 23: System-level test apparatus.

shaken vertically by a servohydraulic actuator mounted to the floor beneath the platform. The shaker, not part of the deliverable AS/VIS system, has a dynamic force rating of 2000 lbf and a bandwidth of several hundred Hz, depending on load dynamics. It can operate in either displacement control or force control modes but cannot operate in acceleration control. For AS/VIS testing, it is limited to displacement control because of space limitation which prevent mounting a load cell between the hydraulic shaker and the platform.

Figure 3 shows the entire AS/VIS system set up for testing. Acceleration sensors described in Section 2.5.1 are mounted on the platform and simulated payload. The electronics rack is visible on the right in the photograph. Cables around the side of the platform are for the sensors and actuators. Each vertical airmount and horizontal actuator is controlled through a single electrical cable. Horizontals have a two compressed air lines, one for air bearings and one for cooling air (the latter has proven unnecessary and will be deleted in flight systems). Verticals have three air lines: one for bearings, one for cooling jets, and one for the air piston. The air piston line runs to the accumulator tank mounted under the platform rather than to the airmount itself. Pneumatic controls for the air piston are mounted in the control rack. All other air controls are in the console mounted to one end of the platform.

The servohydraulic shaker can be positioned in different locations under the platform to accentuate plunge, pitch, or rolling motions. All data shown here had it centered under the platform to accentuate plunging.

3.3 System-Level Isolation Tests

Figure 24 shows schematically the arrangement for system level testing. The platform is shaken vertically by the servohydraulic actuator. The payload weight is 1420 lbs and all actuators are operating with simple negative displacement feedback. Loop gain (stiffness) of the vertical actuators is set to 24 lbf/inch and horizontals to 25 lbf/inch. These values correspond to calculated isolation corner frequencies of 1.05 Hz for the vertical plunge mode and 1.26 Hz for both horizontal translation modes.

Signals from the various accelerometers are processed by an eight-channel digital Fourier analyzer (Zonic Model WCA). Typical measurements include the spectra of acceleration and the ratios of Fourier amplitudes of acceleration on the payload and on the bench.

It is important to note that the aforementioned ratio of Fourier amplitudes is not truly a transmissibility function. The vibration at a specific point on the payload is not entirely caused by the vibration at a single point on the platform. Rather, they are both caused by input force from the shaker which is not measured directly. The distinction is important because, even at low frequencies, the platform has six degrees of freedom. Acceleration ratio measurements will vary somewhat depending on the shaker location and on the choice of accelerometer pair used to form the ratio. Such

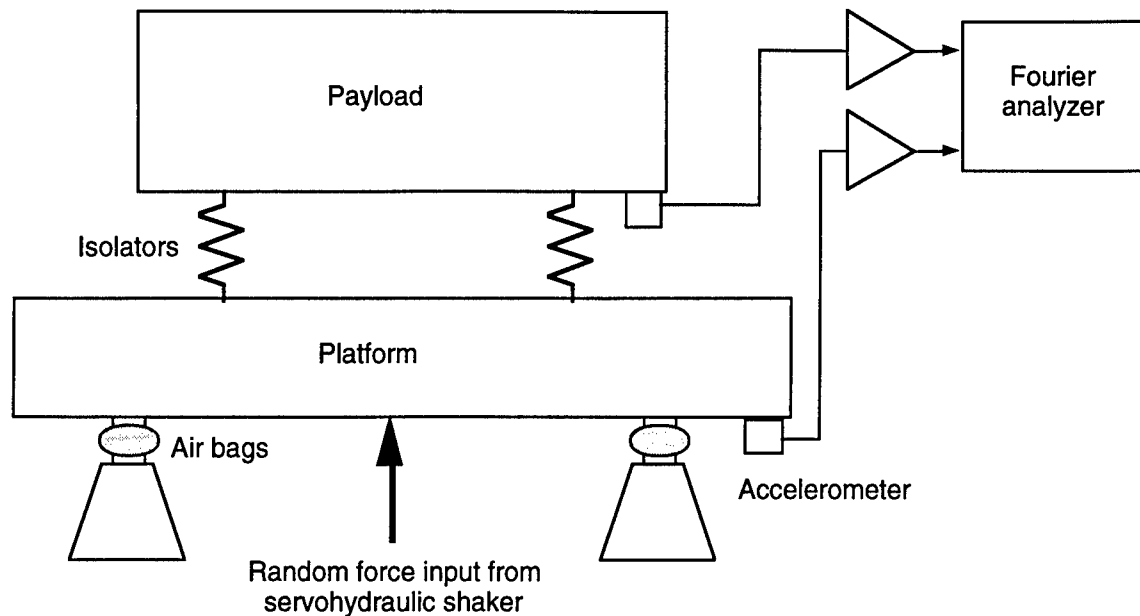


Figure 24: Test setup schematic.

output ratios are still valuable indicators of isolation system performance but they are not entirely system properties. They are affected to some extent by decisions which must be made by the tester. In analysis, the problem would be solved by computing a six-in, six-out frequency response matrix and reducing it to a single function of frequency by singular value decomposition. The experimental counterpart of this process is not practical because of limitations in excitation hardware.

Figure 25 shows the results of a typical system-level test. Accelerometers FZ1 on the platform and BZ1 on the payload are used (Figure 14). Excitation is vertical and near the center of the platform. The exciter is operating in displacement control with a command signal that is random with a flat spectrum from 0.5 to 40 Hz. The left plot shows spectra from FZ1 and BZ1 and the right plot shows their ratio, calculated as a frequency response function (FRF). That is, the FRF is obtained as the ratio of cross power between the two signals divided by the autopower of FZ1 with both numerator and denominator estimated by ensemble averaging. The spectra are in units of rms acceleration per spectral line. This is obtained by multiplying the acceleration power spectral density by the analyzer resolution bandwidth and taking the square root.

Points to note regarding this measurement are follows.

- The isolator corner frequency is not clearly visible in the FRF. This is due to poor coherence between the signals at low frequency caused by the fact that a flat displacement spectrum produces little input acceleration at low frequency. Nonetheless, the rolloff between 2 and 20 Hz makes it clear that the corner frequency is slightly over 1 Hz.
- Isolator rolloff is only visible up to about 25 Hz. Above that, response on

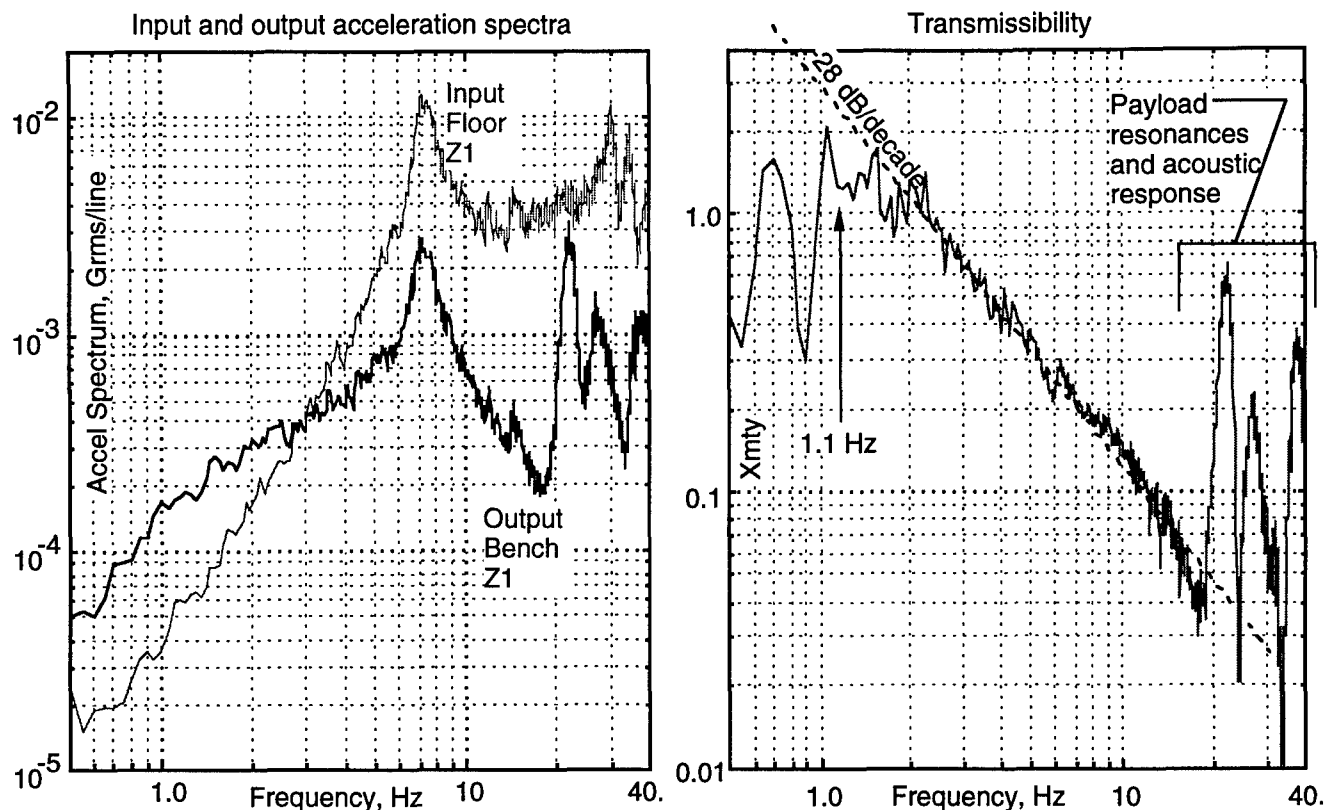


Figure 25: 0.5-40 Hz system-level test results.

the payload is amplified greatly by lightly damped resonances of the payload itself. Acoustic excitation of the payload also becomes significant at higher frequencies. Both effects are common problems in isolation, even though they are independent of the isolators themselves. For now, their importance is that they mask the isolator performance. The eventual solution will probably be structural improvements to the test payload to increase its stiffness.

- The rolloff is slower than predicted, about 28 dB per decade. This casts suspicion more on the measurement itself than on the isolators, as will be shown in later data.
- The platform acceleration shows a distinct peak at about 7 Hz. This is not the suspension resonance frequency but is produced by the combination of platform dynamics and the characteristics of the shaker control system. It is not entirely unwelcome since the true airframe floor acceleration may well have peaks in this range due to wing bending modes, etc.

The main conclusion from this test was that a better test was needed. After some discussion, it became clear that the basic problem is with the input (platform acceleration) spectrum. It has so much energy at higher frequencies (above 10 Hz) that measurements in the important low frequency range are being clouded. Further

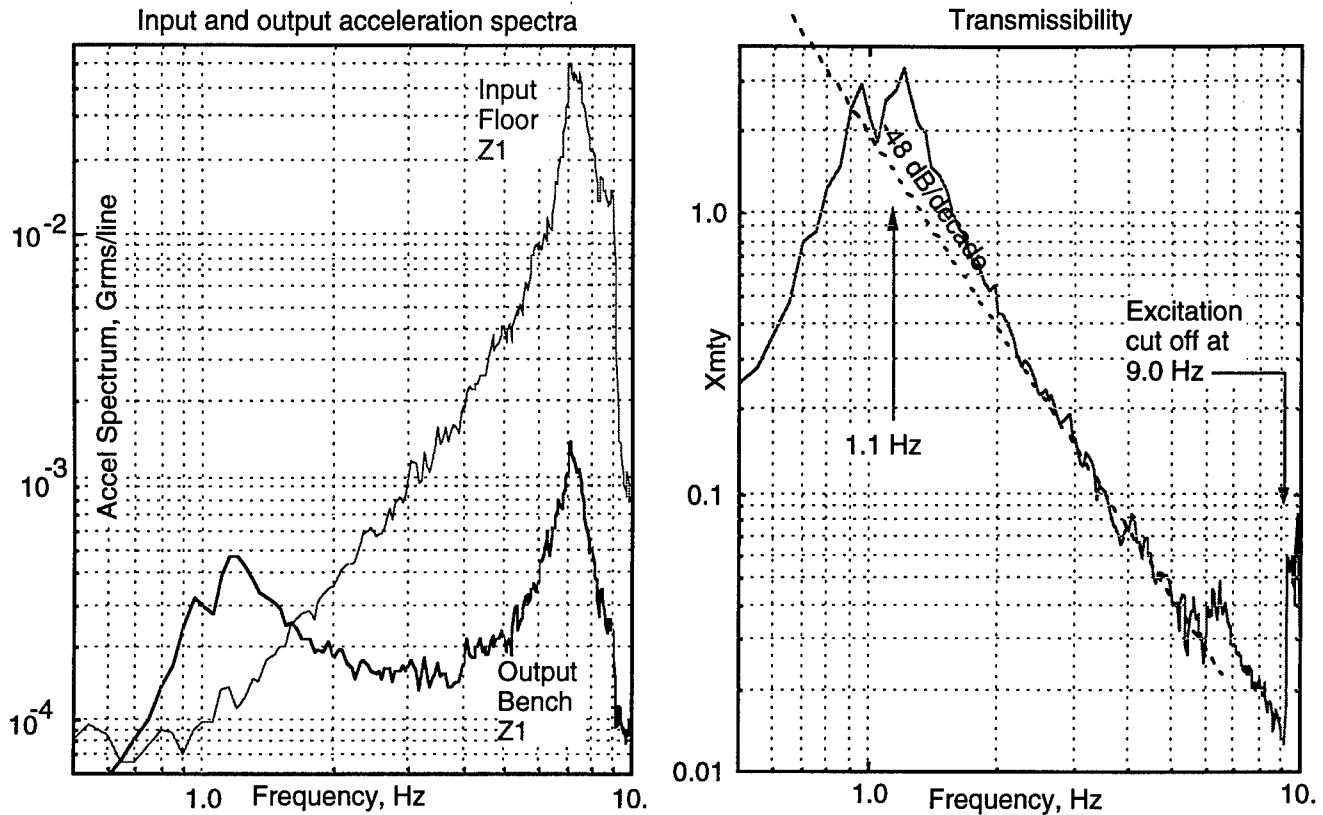


Figure 26: 0.5-9.0 Hz system-level test results.

tests were therefore run with the input spectrum lowpass filtered to 0.5 to 9.0 Hz. Results are shown in Figure 26. Format is the same as in Figure 25.

As expected, this measurement gave much improved (though not perfect) coherence in the 1-9 Hz range. The break frequency is now clearly evident at 1.1 Hz, in good agreement with the predicted value of 1.05 Hz. Rolloff is much closer to the expected value of 40 dB/decade. The input acceleration spectrum is still not adequate at very low frequency (below 1 Hz). The FRF amplitude must approach unity as frequency approaches zero but the test input was not adequate to show this trend. Such a very-low-frequency test is probably impossible with the existing test setup because of the stroke limit on the air bag mounts for the platform.

3.4 Other System Level Tests

A quite different test was performed to provide a simple, highly visual demonstration of AS/VIS performance. Two pencil lasers were mounted on the test apparatus, one on the platform and one on the payload. The shaker was mounted under one end of the platform to produce significant pitching motion as well as plunging. A sinusoidal signal of 10 Hz was input and the amplitude was adjusted to give a vertical acceleration of about 0.5 G peak at the end of the platform over the shaker. This level is quite severe, and would make it highly uncomfortable for a person to sit on

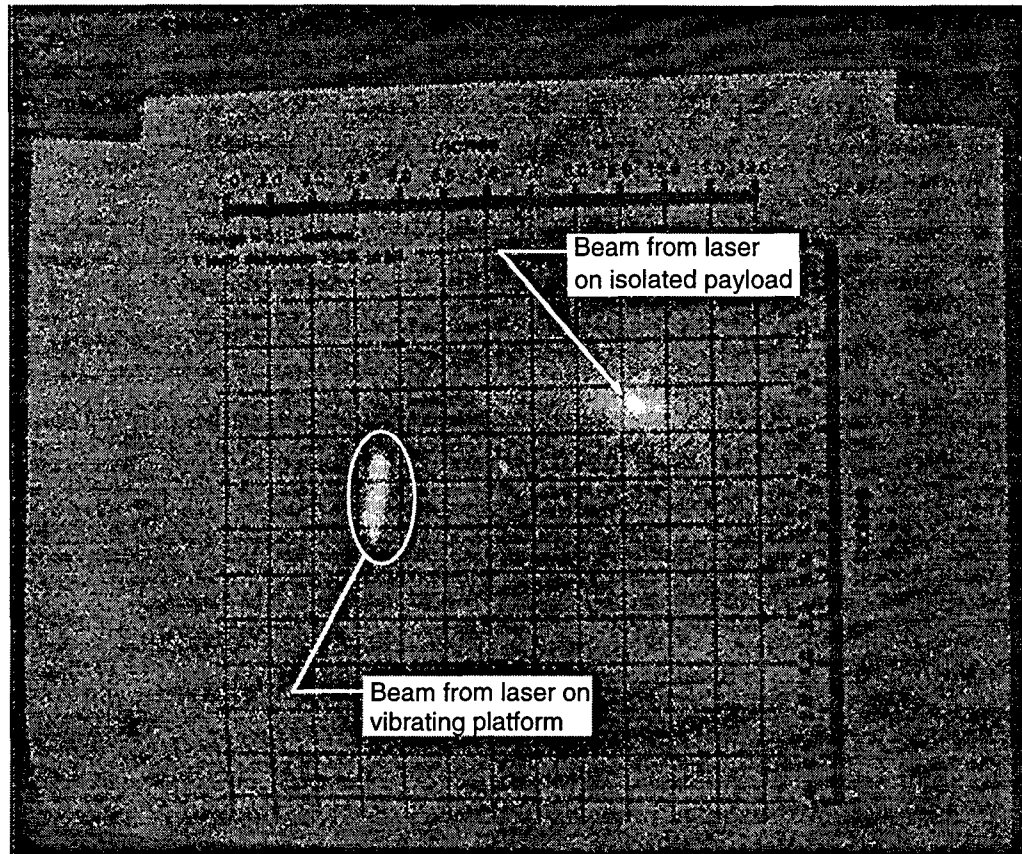


Figure 27: Laser beams from platform and payload under 10-Hz sine excitation.

the platform.

Both laser beams were projected on a paper target about 25 feet away. Figure 27 shows a photo of the laser spots. The spot from the payload laser stands virtually still while the other oscillates over a distance of about 1.5 inches. Figure 27 does not entirely convey the effect because of difficulties in photography⁹ but in person, the demonstration is quite dramatic.

3.5 Component-level Isolation Tests

System-level testing of AS/VIS demonstrated vertical isolation of nominally -40 dB at 10 Hz with an attenuation slope of slightly over -40 dB per decade in the range from 2 - 10 Hz. This is consistent with design analysis. While obviously necessary, system-level isolation measurements are limited by resonances of the dummy payload which begin in the 20-25 Hz range. However isolation performance at higher frequencies, around the resonances of an actual ABL payload, is very important. These resonances are expected to be in the 40-100-Hz range. While the existing

⁹The lasers were not of equal power. An exposure that captured the dimmer, moving image from the platform laser made the image from the brighter stationary, payload laser tend to bloom into a large spot.

dummy payload could be rebuilt to increase its natural frequencies somewhat, it is not feasible to make it dynamically similar to an actual ABL optical bench.

An attempt was therefore made to measure the isolation performance of a single airmount supporting a payload. The motivation was that the single-unit payload could be much more compact and dense than the dummy optical bench structure used in system tests (Figure 23) and would therefore have higher natural frequencies. This would extend the usable test frequency range. Component-level tests were done after all contractual funds had been expended and were necessarily limited in scope. Nonetheless the situation presented the best opportunity to date to characterize the regulated pneumatic springs which are the heart of the AS/VIS system. With a modest amount of follow-on support from Team ABL, component-level tests were performed on the vertical airmounts. Vertical isolation was of primary concern because it is obtained through pneumatic springs that cannot be completely modeled from first principles. Horizontal isolation is achieved through linear metal springs with active augmentation for damping. It is inherently more predictable by analysis and was therefore not the subject of these follow-on tests.

A secondary objective of component testing was to benchmark the behavior of a pneumatic spring for various sizes of its accumulator tank. While the effect of tank size is easily predicted for an air spring without inflow or leakage, the real case is more complex and depends on the behavior of the pressure regulator. Tests of a single isolator presented an opportunity to investigate such effects at minimal cost since only a single tank had to be changed.

3.5.1 Test Method

Two test methods are possible, as shown in Figure 28. In both cases, a known test weight is supported by the isolator under test. The weight is constructed to make its natural frequencies high relative to the upper limit of the test band. The differences between the two methods are explained below.

In the first method, called a direct transmissibility test, the isolator under test is placed on a moving platform which can be shaken vertically such that a controlled base motion is produced. Vertical accelerations on the base and on the payload are transduced. The frequency response between the former and the latter is measured under random base motion input. This function, called $\hat{H}(f)$, is the desired transmissibility with no further processing required, hence the designation "direct" test.

In the second method, called an indirect transmissibility test, the complex stiffness of the isolator is measured via an admittance test and used to calculate transmissibility. The isolator under test is mounted to rigid ground and a measured time-random vertical force is applied to the payload mass. In the present case, the integral actuator of the isolator itself would be used for excitation with force inferred from coil current. The frequency response $H_a(f)$ between input force and vertical acceleration on the payload is measured. It can easily be shown that, for this 1-DOF system:

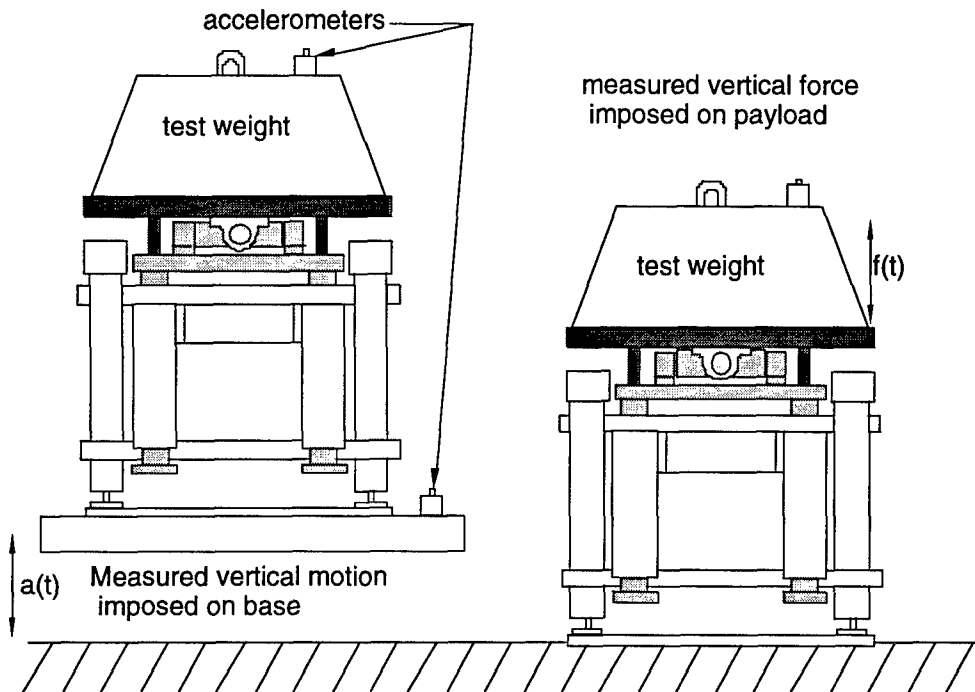


Figure 28: Direct (left) and indirect (right) methods of testing isolator transmissibility.

$$\hat{H} = 1 - mH_a(f)$$

where m is the mass of the test payload including the moving element of the isolator. This simple relation allows indirect determination of the transmissibility function \hat{H} via the measured admittance function H_a .

The indirect method is less expensive because almost no fixturing is required. Its disadvantages relate to error sensitivity. As frequency f increases, $H_a(f)$ approaches $1/m$ and \hat{H} becomes smaller and smaller. But \hat{H} is obtained by subtraction of two nearly equal terms. In the range of interest here, \hat{H} is very small compared to unity (on the order of 0.01) so a small percentage error in either m or $H_a(f)$ can produce a large percentage error in \hat{H} . This implies that the measurement error in $mH_a(f)$ must be small compared to the expected value of \hat{H} in the frequency range of interest. Therefore the error in m or $|H_a(f)|$ must be of order 0.1% or less and phase error of $H_a(f)$ must be of order 0.001 radian or less. Such levels of accuracy cannot be reliably obtained within the scope of this testing. Hence the indirect method, for all its elegance, would not satisfy the objectives.

The conclusion is that the indirect method may be useful at low frequencies where isolation is less than about 20 dB but definitely not where it approaches 40 dB. The actual borderline will depend on what calibration accuracy can be achieved, both in acceleration and force sensing. The direct method is the clear choice for the regime

of main importance here.

3.5.2 Test Apparatus and Procedure

The apparatus for conducting a direct transmissibility test is shown in Figure 29. A controlled vertical motion is imposed on the base of the airmount under test by a second identical airmount supporting the first as shown. In effect, the lower airmount is used as a shaker for testing the first. The airmounts are actually well suited for use as low-frequency, low-amplitude shakers. The air spring provides soft support for the weight of the test article and the actuator provides up to about 65 lbf rms force (200 lbf peak random) without forced air cooling. The low stiffness of the air spring allows almost all the coil force to be reacted into the inertia of the payload.

The air piston easily supports the 146-lb weight of the isolator under test plus its payload of up to several hundred pounds. Base acceleration levels of 0.1-0.2 G rms, consistent with expected in-flight levels, are available. Perhaps best of all, the relatively simple apparatus was constructed at low cost and allowed the tests to be performed in CSA's own lab. This was key to completing the component tests since using an outside, commercial shaker facility would have exceeded the budget.

Both lower and upper airmounts were modified by adding a machined load plate to the top of the flexure U-joint as shown. The plates include steady legs which brace against the carriage crossmember to hold the plate level. The plate allows a weight to be supported by a single isolator. It also provides alignment such that the weight c.g. can be accurately positioned over the center of the airmount carriage. The "stack" of two isolator/actuators plus test weight were positioned under a gantry with a chain hoist for handling the test weight. A noncontacting safety loop was used around the lifting bar of the test weight during testing.

A vertical airmount/actuator provides both vertical and horizontal isolation. However its design allows the horizontal isolation to be locked out without affecting the vertical (Figure 5). Both upper and lower airmounts in Figure 29 were configured in this way for testing.

3.5.3 Instrumentation

In theory, the displacement sensors built into the two isolators would be sufficient for measuring transmissibility. In practice, this would lead to accuracy limitations due to subtractive cancellation error, just as in the indirect test method. Therefore accelerometers were used on the moving base platform and test weight platform as shown.

The test required only two accelerometers, both measuring in the vertical direction. These were mounted on the undersides of the two load plates as shown. The accelerometers were Wilcoxon Model 731A's with matched P31 power supply/couplers. These seismic accelerometers can measure from below 0.2 Hz to above 100 Hz with

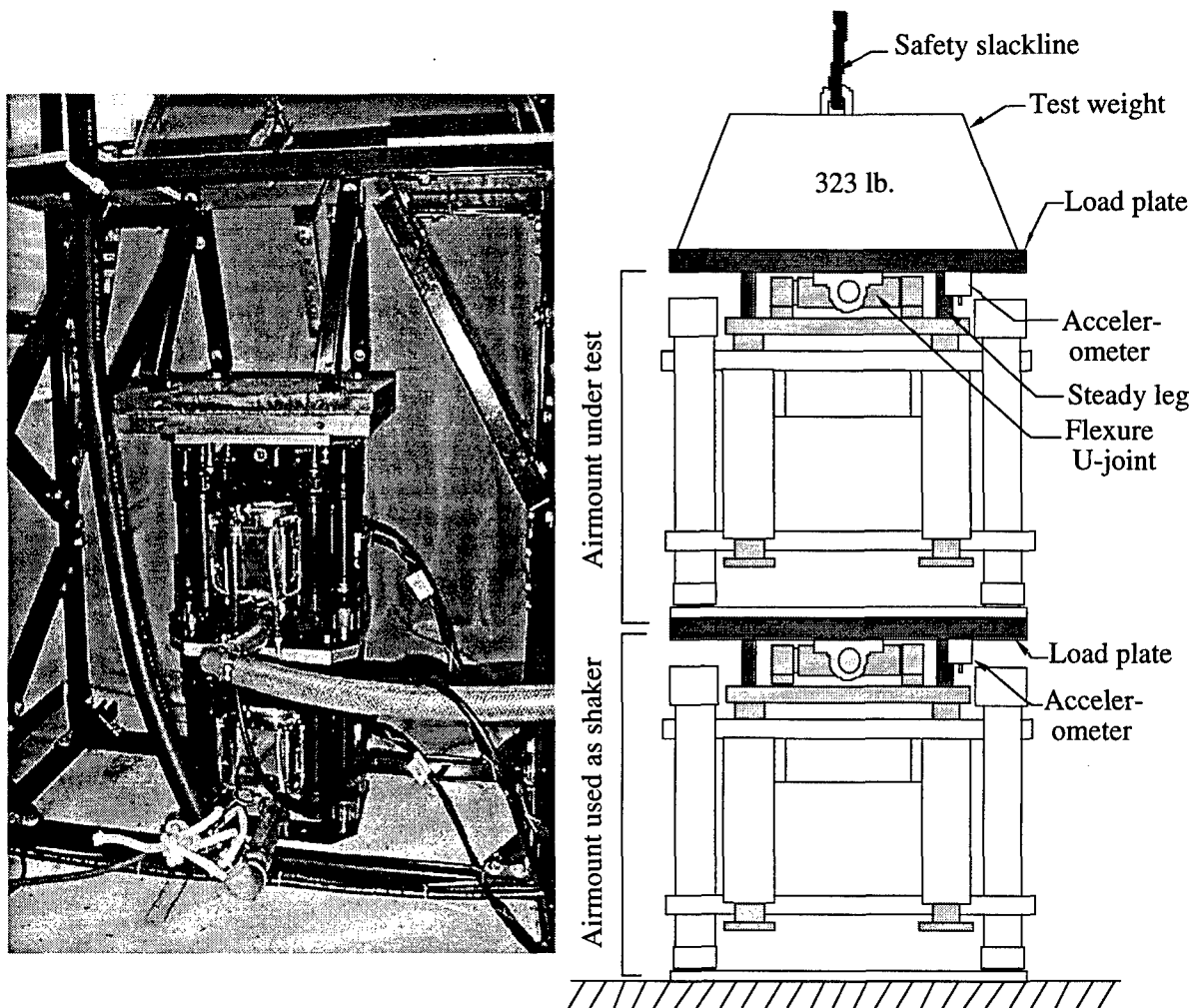


Figure 29: Test apparatus for single-unit vertical transmissibility testing. Device carriages are shown in light grey and load plates in darker grey.

a noise floor of less than one micro-G and maximum input of 0.5 G. They were well suited to measurements over the entire frequency and amplitude ranges of interest.

Because the transmissibility tests are direct, relative error in the final result is no worse than in the transducer calibrations themselves; subtractive cancellation error is not a factor. Data acquisition was done by a Zonic Model WCA Fourier Analyzer. Data was converted to MatLab format for display and inclusion in this report.

3.5.4 Test Procedure

Test procedure consisted of the following steps.

1. The airmount under test was configured with the desired combination of payload, accumulator tank, and active loop gain.
2. Pressure in the piston of the lower airmount (Figure 29) was adjusted to float its load, namely its carriage, load plate, the upper airmount, its load plate, and the test payload.

Tank size	2 gal.		7 gal.		30 gal.	
Payload, lb.	323	165	323	165	323	165
Active gain lbf/inch	24.3	4.86	10.8	4.86	6.08	4.86
		24.3				

Figure 30: Test matrix for component-level isolation tests.

3. The displacement loop of the lower airmount was closed with a gain of 24.3 lbf/inch and its carriage was allowed to settle to the center of its vertical stroke.
4. Pressure in the piston of the upper airmount was likewise adjusted to float its load.
5. A band-limited random signal was input to the power amplifier of the lower airmount. Bandwidth was nominally 0.1-70 Hz. Input amplitude was adjusted to just below that which would cause the carriage of the lower airmount to hit its travel stops.
6. Signals from accelerometers on the upper and lower load plates were connected to a Fourier analyzer and transmissibility was measured using the lower airmount carriage acceleration as the denominator. 800 spectral lines were measured over 0-50 Hz with 12-20 records per ensemble, Hanning window, and 50% overlap.
7. Data saved from each run included sample time histories (the last 2048-point block from each ensemble for each channel), spectra for each channel in units of G (rms) per spectral line, transmissibility, and ordinary coherence between the two channels.

Tests were run for a total of seven combinations of payload, accumulator tank size, and active displacement loop gain. The test matrix is shown in Figure 30.

A background noise measurement was also made for the configuration given by the rightmost column in Figure 30. This was done by executing the steps of the procedure given above except for step 5. The random input signal was replaced by shorting the input to the power amplifier. All full-scale levels on the analyzer A/D converters were left at their normal settings. The sample time histories and spectra were saved as measures of the background noise.

3.5.5 Results

Figure 31 shows transmissibility functions measured with a payload of 353 lbs (including load plate) and three different tank sizes. In each case, the active displacement-loop stiffness was set to approximately the value that would be used with that tank size. As the tank is made larger, a lower value of active stiffness would typically be used to take advantage of the reduced pneumatic stiffness.

Several observations can be made regarding these measurements.

- They are rather noisy. Coherence is low over the entire frequency range and is particularly poor below about 1.5 Hz.
- Rolloff rate drops to only about 20-25 dB/decade by about 5 Hz.
- An isolation floor of about -30 dB is present.

The cause of these disappointing results was traced to a slight friction drag in the air bearings. After some experimentation, it was determined that this was caused by the load plate. It tends to impose bending moment on the crossmember of the device carriage to a greater degree than does the normal load interface. This deflects the bearing journal rails (Figure 5) very slightly out of parallel and causes the radial load on the lower bearings to exceed the level that can be carried by the air film. This effect is probably present with the normal load interface but to a lesser extent: bearing friction will occur eventually as load is increased but the onset will occur at a higher load. Later version of the airmounts will use a modified carriage design with a smaller U-joint footprint and an added lower crossmember below the magnet body. These changes should largely eliminate the load-limit problem.

Payload was reduced to 195 lbs, a value below the friction threshold, and the tests were repeated. A low value of active centering stiffness was used for all tests to highlight the properties of the air spring. Results are shown in Figure 32. The isolation floor is now about -40 dB and coherence is much improved. The rolloff rate is essentially the same for all three tank sizes: -56 dB/decade. While this fast rolloff is certainly welcome, no explanation has been found as to how a passive device can exceed -40 dB/decade.

In all the tests shown in Figure 32, the transmissibility increases above the -40 dB floor at higher frequencies, starting at about 14 Hz. Two facts suggest that this is an artifact of the test apparatus: (1) the behavior is almost independent of isolator stiffness (tank size), and (2) there is no physical reason why the stiffness of damping of the isolator should increase at higher frequencies. The rise is probably due to resonances of the test fixturing. While the component-level tests have yielded important information, they have not answered the question that motivated them: what are the characteristics of the airmount in the higher frequency range from 20 to

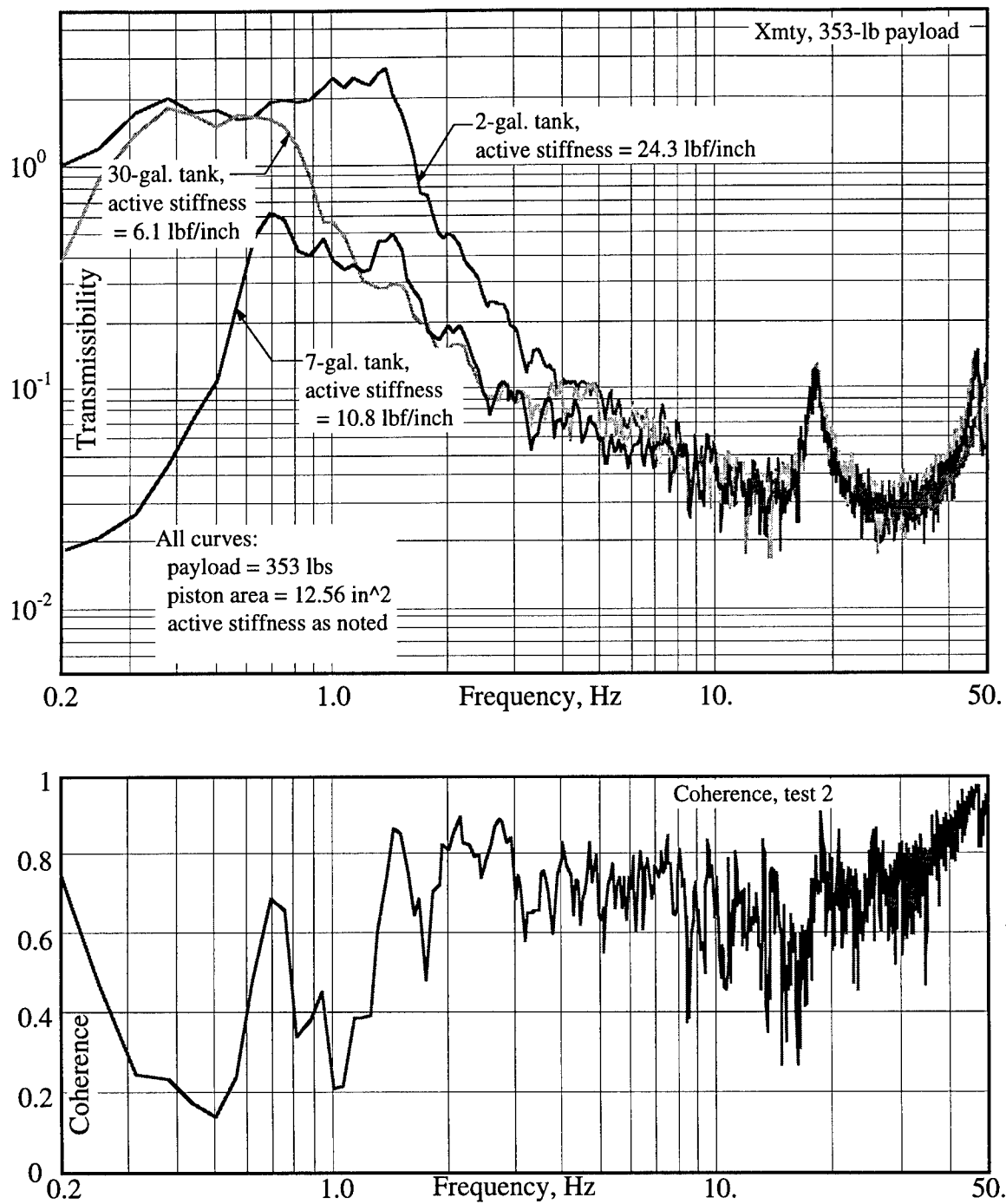


Figure 31: Measured single-dof transmissibility with 353-lb payload.

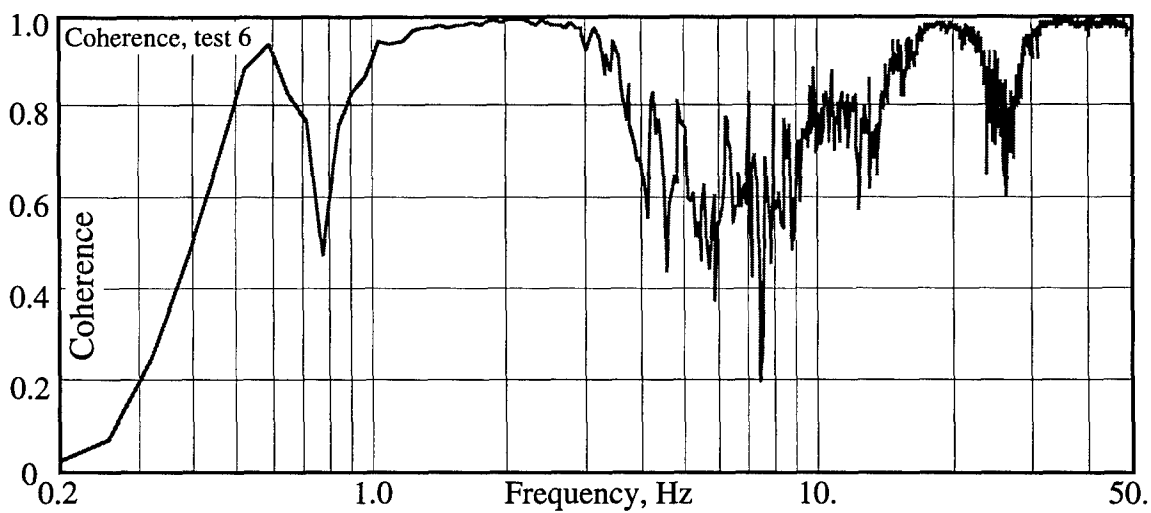
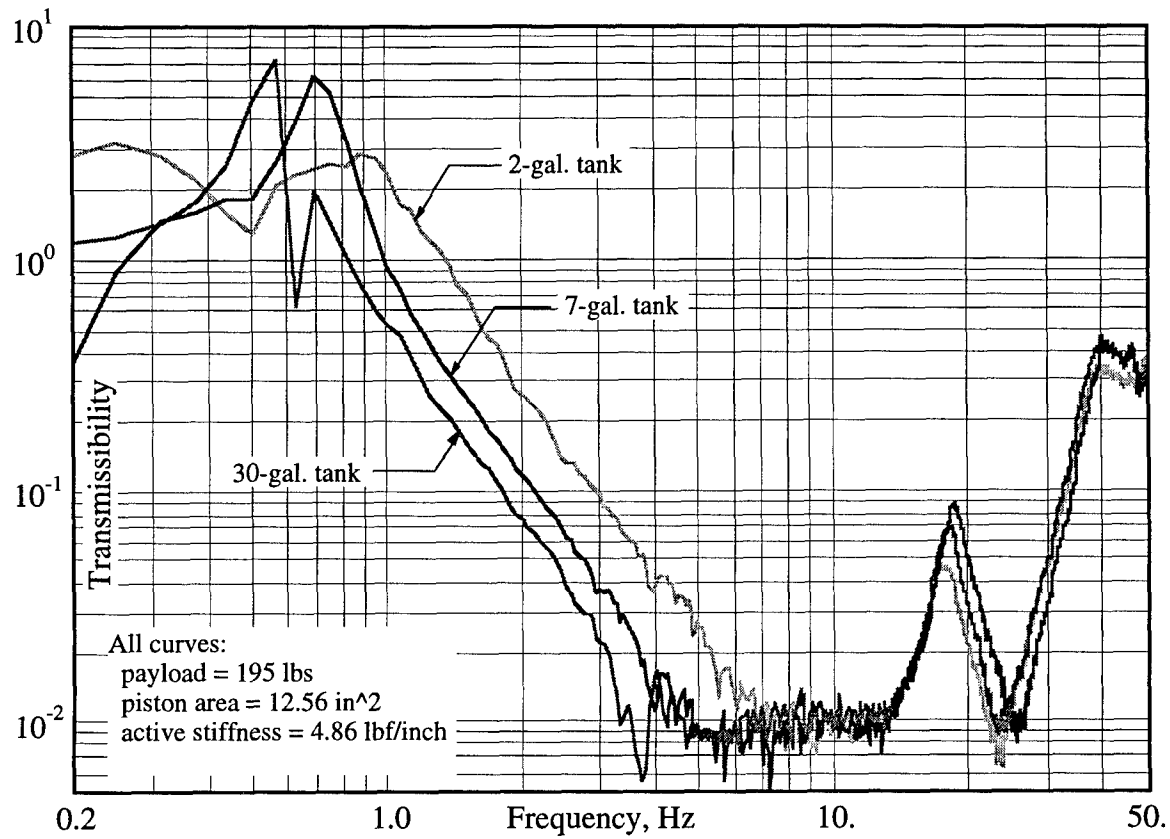


Figure 32: Measured single-dof transmissibility with 195-lb payload.

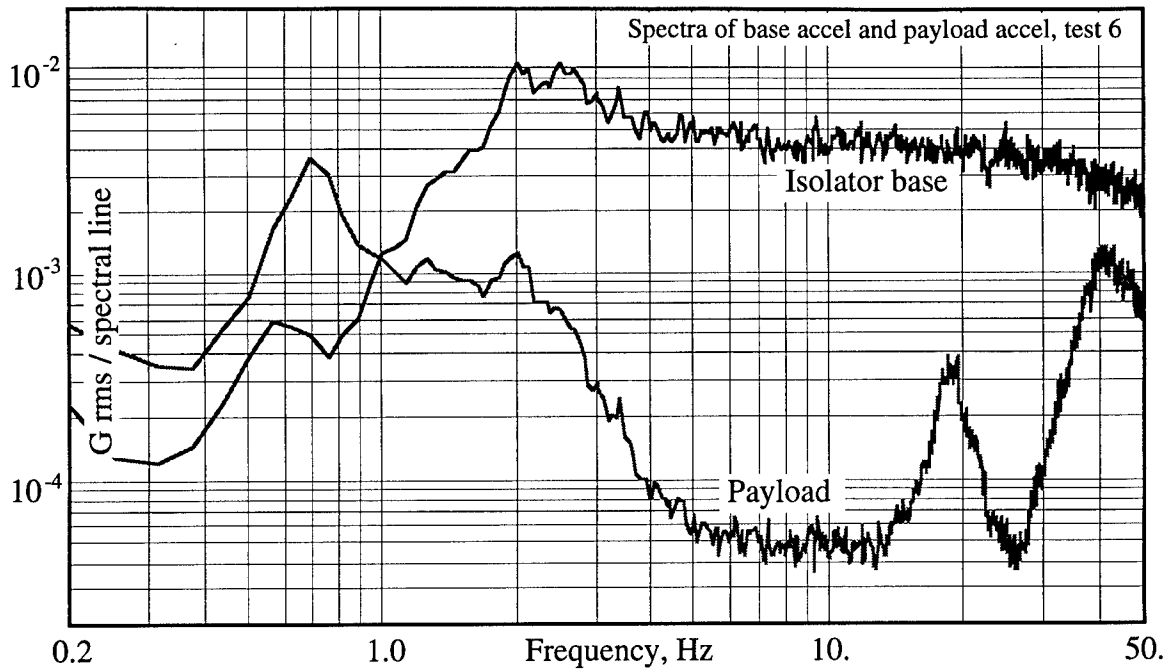


Figure 33: Typical input and output acceleration spectra from component transmissibility tests.

100 Hz. This question will be revisited during development of flight versions of the AS/VIS system for Airborne Laser¹⁰.

Even when no friction is present, the input/output coherence across the isolator is poor for very low frequencies, below about 0.4 Hz. This is caused by the fact that the base acceleration spectrum drops off sharply for frequencies below about 1 Hz, as shown in Figure 33¹¹. The rolloff occurs because, at frequencies below the vertical resonance of the lower airmount (about 1 Hz), most of the force input to the coil is reacted by into the stiffness of the mount, rather than into the inertia of its payload. As often happens in frequency response measurements, the usable frequency range of the FRF is determined by limitations on the ability to control the spectrum of the denominator function.

Figure 34 shows a comparison of suspension frequencies from Figure 32 with calculated values. The latter account for both the stiffness of the air spring, per Figure 1,

¹⁰The work described in this section on component-level tests was funded by Team ABL and was performed after the draft report had been submitted. Prior to submission of the final draft, it was announced that Team ABL had won the Airborne Laser competition. This means that AS/VIS is part of the winning baseline design, and that development to flight versions will continue under the ABL contract.

¹¹Each of the two functions in Figure 33 is the square root of an acceleration power spectral density multiplied by the square root of the measurement frequency resolution. Ordinate units are thus g's (rms) per spectral line.

Test number	5	6	7
Tank size, gal.	30	7	2
Total volume, cu. in.	7002.	1696.	542.
Piston area, sq. in.	12.56	12.56	12.56
Total piston load, lbs*	225.	225.	225.
Active stiffness, lbf/inch	4.86	4.86	4.86
Calculated freq., Hz.	0.93	0.66	0.54
Measured freq., Hz.	0.90	0.70	0.57

* Includes carriage, load plate, and test weight

Figure 34: Calculated and measured vertical suspension frequencies.

and the active displacement loop stiffness of 4.86 lbf/inch. Agreement is quite acceptable.

3.6 Test Conclusions

Overall, the AS/VIS system performance was considered satisfactory. It demonstrated the feasibility of very soft passive pneumatic supports integrated with high-force, long-stroke voice coil actuators for active control.

Component-level test results demonstrated passive vertical isolation performance of -40 dB at frequencies as low as 4 Hz. Amplification at the suspension resonance as low as 9 dB was also demonstrated. This performance is well beyond the current state of the art for laboratory isolators of comparable payload and stroke, even before any active augmentation is used.

System-level performance results were consistent with those at the component level, although limitations in the test apparatus complicated their interpretation. Improvements in the system-level test apparatus and procedure are clearly needed to display the full capability of the system. Primary among these are the following.

1. The servohydraulic actuator should be reconfigured to provide a much flatter acceleration spectrum on the platform. This could be done most practically by shaping of the displacement command signal, either analog or digitally, to give a 40 dB/decade rolloff starting at about 1 Hz.
2. The air bag springs supporting the platform should be replaced with others having longer stroke and lower stiffness. Besides making the platform acceleration control problem easier, this would allow isolation testing with a small fixed

pitch or roll angle imposed on the platform. This would be useful in testing certain control laws such as acceleration feedforward.

3. The simulated optical bench payload should be reworked to increase its own natural frequencies. This would allow system-level isolation testing over a wider frequency band.

The last of these items is particularly important. A primary function of the isolation system is to suppress excitation forces on the optical bench payload in the frequency range of its first few natural frequencies. These will be substantially higher than the 20-25 Hz range of the existing dummy payload. To demonstrate isolation in the 30-40 Hz range, for example, the first modes of the payload must be above about 45 Hz. In effect, the dummy test payload must be dynamically stiffer than the actual optical bench in order to verify performance of the isolators.

4. Control Laws

The objective of this SBIR project was to produce a demonstration system that could be used, among other things, for development of control laws and algorithms for active vibration control. Such development was not itself a primary objective of the SBIR. Nonetheless some work was done in this area simply to shake out and demonstrate the digital control system and the software development facilities. Likewise, some baseline control scheme was necessary for setting goals and requirements for the sensor and actuator hardware. This section describes the baseline control method.

A fundamental problem in airborne isolation is the presence of near-DC inertial forces imposed on the payload during aircraft maneuvering. The Airborne Laser 747 for example, will patrol in a figure-8 pattern, with long, constant-radius turns at either end. The effective G force on the payload will be greater during the turns than during the straight sections of the figure-8. This could cause significant sag of a payload supported on the soft mounts, pneumatic or otherwise, needed for high isolation. Counteracting this effect is a natural application for the active subsystem of the AS/VIS.

4.1 Acceleration Feedforward

The obvious control scheme for this purpose is filtered acceleration feedforward. DC-coupled accelerometers on the aircraft floor sense its acceleration, both rigid-body and flexible-body. Signals are lowpass filtered to eliminate flexible-body components and then used in an algorithm that calculates the required forces at the actuator degrees of freedom to make the payload DC acceleration match that of the airplane in all six degrees of freedom. These force commands are then sent to the actuators. Negative displacement feedback is also used to make the active system behave like a set of six springs connecting the payload to the aircraft floor. This is necessary at least in the local vertical direction since the pneumatic isolators have no DC stiffness of their own.

A system of active springs with digital control has numerous advantages over passive. Among them is the fact that translational and rotational stiffnesses need not be interdependent. Roll stiffness can be introduced, for example, without affecting plunge stiffness and vice versa.

Acceleration feedforward reduces the stroke requirement of the isolators, an important consideration when the corner frequency must be low to achieve the required isolation. It does so at some sacrifice of isolation but this tradeoff can be optimized through the choice of type, order, and cutoff frequency of the lowpass filter. A block diagram of the control law is shown in Figure 35. A simplified one-DOF version is shown in Figure 36.

Simulation results were computed for the 1-DOF case to illustrate the principle.

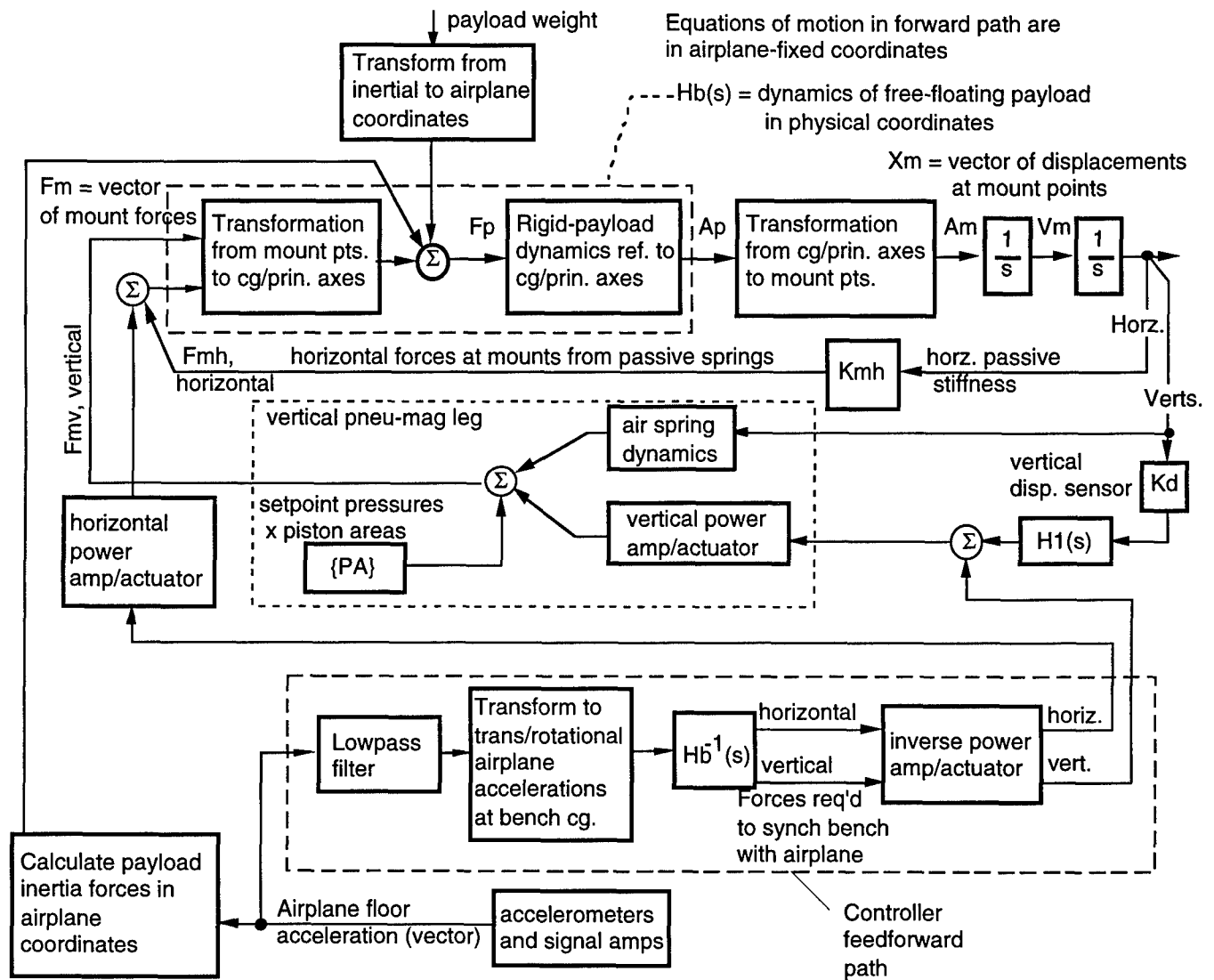


Figure 35: 6-DOF control law using pneumatic airmounts, vertical displacement feed-back, passive horizontal springs, and floor acceleration feedforward.

The input was a stationary random floor acceleration with an rms value of 20 in/sec^2 plus a step of 38.6 in/sec^2 (0.1 G). Results are shown in Figure 37 in terms of payload absolute acceleration and displacement across the isolator. Three isolator types were simulated:

1. A pneumatic isolator with the characteristics of an AS/VIS vertical airmount, 25 lbf/inch active stiffness, 350 lb payload per isolator, and acceleration feedforward. The lowpass filter is a 4-pole Butterworth with 1.0-Hz cutoff.
2. Same as (1) without acceleration feedforward.
3. A linear spring-dashpot isolator with suspension frequency of 3.0 Hz, damping of 10% of critical, and no acceleration feedforward.

Results in Figure 37 show that the 1.07-Hz pneumatic isolator gives substantially better steady state isolation than the 3.0-Hz passive device but requires much larger stroke to accommodate an acceleration step transient. Adding feedforward reduces the stroke requirement at some cost in steady-state isolation. Besides illustrating the benefit of acceleration feedforward, the example shows why pneumatic mounts need it for use under varying quasistatic load. Referring to Figure 1, an air spring adds dynamic stiffness, which tends to reduce isolation, but not static stiffness, which reduces displacement under static load. An AS/VIS airmount is, in effect, a 1.1 Hz device with respect to isolation but only a 0.66 Hz device with respect to displacement under step load.

4.2 Positive Position Feedback

A second function of the active subsystem would be to add damping to horizontal suspension modes. This is necessary because the mechanism for allowing horizontal motion, the column flexures of the vertical mounts, is nearly undamped. The logical control law here would be positive position feedback (PPF). This involves feeding back position with a positive sign through a 2-pole resonant filter. The filter resonance is tuned to match the frequency of the suspension mode to be damped. The filter provides the 90-degree phase shift required for damping as well as amplification to make the effective damping quite large. Best of all, the filter causes the feedback gain to drop off at higher frequencies where the feedback would otherwise stiffen the system and reduce isolation. The tradeoff again is with respect to sag of the payload under transient step acceleration loads. It would be somewhat increased by PPF which tends to destiffen the system at frequencies below the filter resonance.

4.3 Inertial Stabilization

A third control possibility is inertial stabilization. This amounts to using a payload-mounted, inertially referenced motion sensor as the feedback source. The actuators

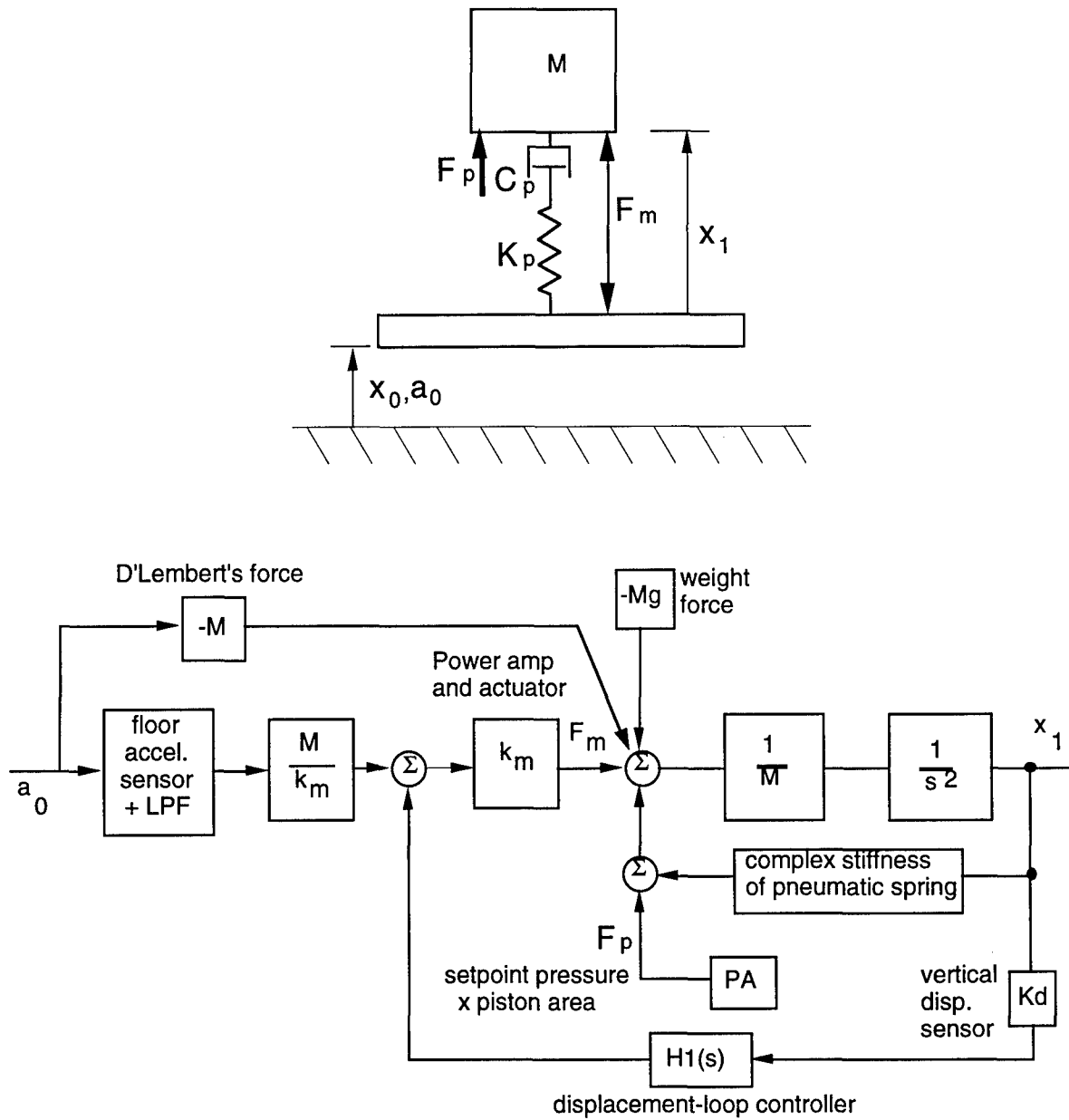


Figure 36: Simplified acceleration feedforward control law for one degree of freedom.

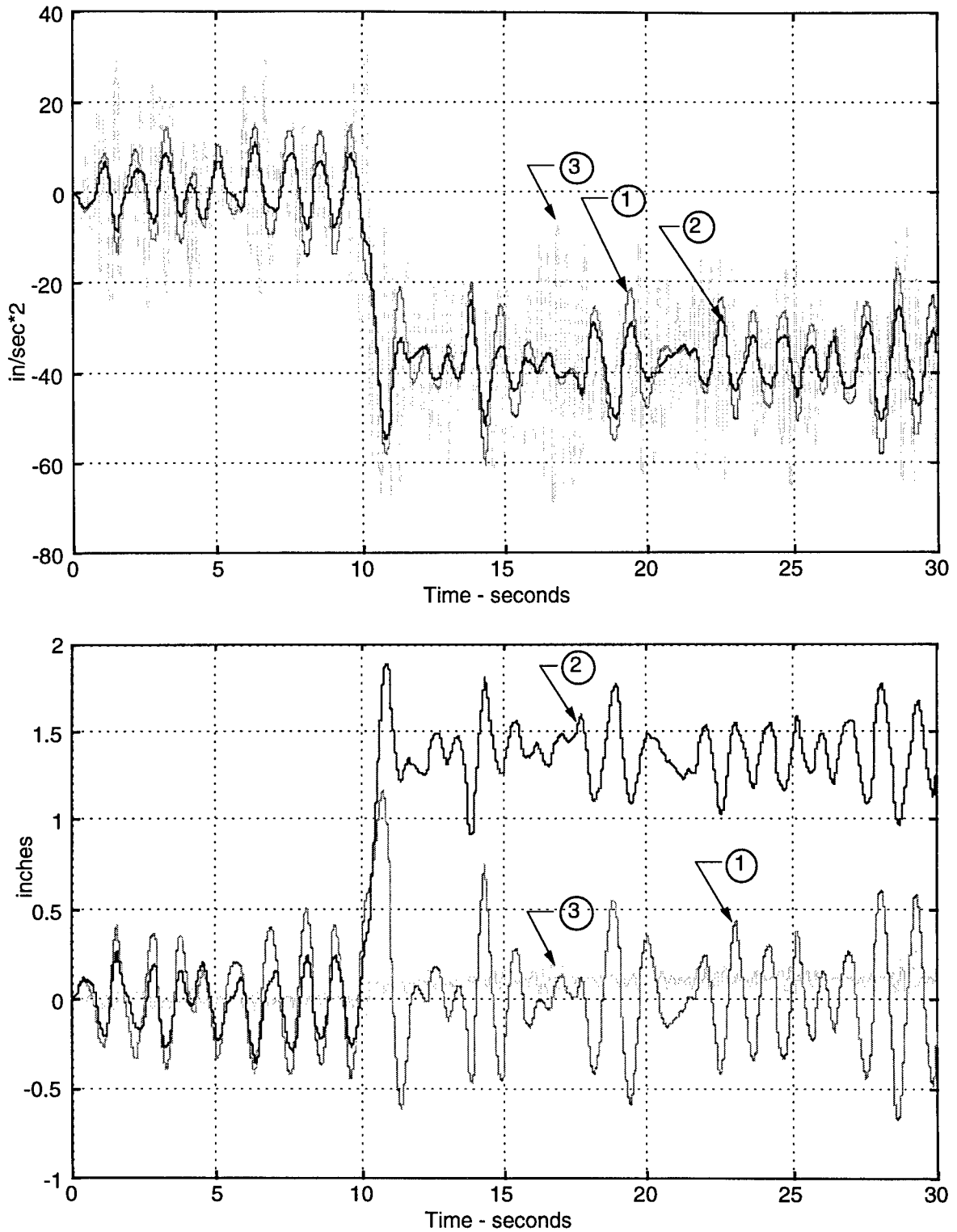


Figure 37: Payload absolute acceleration (top) and isolator displacement (bottom) for three types of isolators. 1 - AS/VIS with acceleration feedforward, 2 - AS/VIS without acceleration feedforward, 3 - 3.0 Hz passive with 10% damping.

are driven in such a way as to attempt to null the output from this sensor. If the sensor produces a signal proportional to displacement, the control is essentially tying the payload to inertial ground through an active spring. If the sensor gives rate, such as a gyro, the tie to inertial ground is through an active dashpot. This approach would be appropriate in cases where the aircraft is flying straight and level and maximum isolation is required. It is similar to the method commonly used for stabilizing gimbal platforms.

The AS/VIS system has been proposed for use on the Airborne Remote Earth Sensing (ARES) project. Managed by Lawrence Livermore National Laboratory, it involves an aircraft carrying an optical bench with sensors looking down at the earth from high altitude. Since the aircraft normally flies straight and level during data acquisition, inertial stabilization would be the most likely control strategy for this application.

5. Conclusions

The development and initial testing of the Airborne Suspension/Vibration Isolation System has been described. Aimed specifically at the requirements of the Airborne Laser, the system is a combination of an advanced pneumatic passive suspension, high-capacity voice-coil actuators, integrated sensors, a flexible, powerful control processor and a commercial system of software development tools.

The deliverable hardware has two purposes. It will serve as a development tool for control laws, algorithms, and software for active isolation, and it will allow efficient continuing development of the front end hardware, eventually leading to flightworthy isolation systems for optical benches of the ABL.

Initial testing of the AS/VIS demonstration hardware has been completed, both at the component and system level. Performance is generally satisfactory although continued development of the test apparatus and method itself is recommended.

5.1 Suggested Future Work

AS/VIS represents a radical jump in vibration isolation technology in response to a specialized requirement. As such, it is not surprising that the two-year SBIR development has brought to light a number of areas for continuing development. In addition to the baseline applications of control law development, the following are recommended.

- **Active pneumatics.** The force requirements for the actuators are set primarily by low frequency maneuvering loads. If all or part of this could be taken over by active pneumatics, system weight and power requirements could be reduced substantially. What is needed is active control of piston pressure with a bandwidth of about 1 Hz and accuracy of a few hundredths of a psi.
- **Adaptive pneumatics.** Operation of an ABL in turbulent flying conditions could require fast, adaptive stiffening of the isolators. AS/VIS-style pneumatic springs could accommodate this using fast-acting solenoid valves to attach or seal off accumulator subvolumes. The demonstration system could be used for fast prototyping and testing of such hardware under realistic operating conditions.
- **Improved coil cooling.** Air-jet cooling of the coils has not proven successful in the initial trials. However only initial testing has been done and several important avenues for improvement have not been explored. Existing AS/VIS hardware could be used to efficiently develop better coil cooling. The first steps are increasing the jet flows and reorienting the jets to improve entrainment of ambient air into the jet. The payoff would be increased thrust/weight ratio for the actuators.

- **Reduced-weight magnetics.** The preceding three items could allow magnetic voice-coil actuators to be made smaller and lighter. This could reduce system weight substantially since the magnetics are the heaviest components.
- **Increased payload capacity.** Experience in component-level airmount testing indicated that the carriage assembly may not be capable of functioning properly at the maximum payload weight which the air piston can lift. Small deformations of the carriage can cause slight friction in the air bearings which degrades isolation. Several measures have been identified by which the carriage could be stiffened without major impact on the rest of the design. While not necessary for ABL (sufficient payload capacity has been demonstrated), this would allow for future growth in payload weight and produce a more balanced design.
- **Characterization of actuators.** Accurate control of the isolated payload requires accurate knowledge of the dynamic response of the actuators themselves. This fairly straightforward task was only touched on in initial testing. Some uncertainty was discovered which could probably be resolved by expanded component-level tests and upgrading of existing models for the actuator and power amplifier.
- **Multi-axis testing.** Cost constraints prohibited testing the AS/VIS demonstrator under full, multi-axis input of the type it will experience in an aircraft. The existing apparatus could be enhanced with a second exciter to provide simultaneous test capability. Likewise, tuning of the excitation spectrum to approximate the actual in-flight floor vibration would provide an important step forward in traceability to true ABL requirements.
- **Enhanced user interface.** As a software-based active system, the operator interface of AS/VIS will be important to its eventual success as part of the ABL. This interface itself deserves further development, a task for which the existing demonstration system is well suited. The intent would be to utilize the existing demonstration host and fast bus-to-bus interface to allow real-time visualization of the state of the system during operation. This would be extremely useful for evaluation during flight-tests in the demonstrator ABL aircraft.

5.2 Evolution to Flight Systems

Finally, it should be noted again that the existing AS/VIS hardware is a laboratory testbed and demonstrator which was not designed for use aboard an airplane. Doing so would have consumed too much of the available resources for important but routine work such as crashworthiness. Evolution to true, ABL-ready flight systems will require enhancements such as the following.

- **Weight reduction.** Reducing the force requirement on the magnetics will be key in this area. Optimization of existing structural elements and utilization of advanced materials too expensive for the demonstrator will also play a part.
- **Integration of electronics.** Existing analog electronics were designed for low cost, ease of use, and flexibility. For this reason, they are based on off-the-shelf commercial circuit boards and testbed-style packaging. Their size and weight could be reduced substantially by a higher level of integration. Likewise a flightworthy system may require a higher level of EMI immunity than the lab system. A/D conversion in the signal conditioning chassis (or even at the sensor) with digital communication to the control processor should be investigated.
- **Crashworthiness** Air Force design rules for airborne systems require that they be capable of withstanding high G loading without tearing loose from their mounts. A typical requirement is 9 Gs static for hard mounted equipment and 18 Gs for equipment that has any free-play relative to the mounting surface. The optical benches on isolators would clearly fall into the latter category. A means must be found for doing so without compromising the high level of isolation provided by AS/VIS. It will probably take the form of a slack-tether arrangement, external to the isolation mounts. As such, it was excluded from the proof-of-concept work to date but must be addressed for the actual ABL.
- **Durability and maintainability.** The laboratory system was not designed to stand the rigors of life on the flight line. While it has proven reasonably robust and reliable, there are numerous improvements needed. In particular, various precision parts of the airmounts and actuators must be protected from mechanical damage. While straightforward, this work is essential to producing flightworthy systems. Likewise a flight design must address the question of modular replacement on the flight line.
- **Supporting systems.** AS/VIS operation depends on a supply of clean, dry compressed air at about 120 psig. The means for providing this aboard an aircraft with minimum weight penalty must be found.

DISTRIBUTION LIST

AUL/LSE Bldg 1405 - 600 Chennault Circle Maxwell AFB, AL 36112-6424	1 cy
DTIC/OCP 8725 John J. Kingman Rd, Suite 0944 Ft Belvoir, VA 22060-6218	2 cys
AFSAA/SAI 1580 Air Force Pentagon Washington, DC 20330-1580	1 cy
PL/SUL Kirtland AFB, NM 87117-5776	2 cys
PL/HO Kirtland AFB, NM 87117-5776	1 cy
Official Record Copy PL/VTV/Eugene Fosness Kirtland AFB, NM 87117-5776	2 cys
PL/VT Dr Hogge Kirtland AFB, NM 87117-5776	1 cy